BULLETIN
DE
L'ACADÉMIE POLONAISE DES SCIENCES

Rédacteur en chef
K. KURATOWSKI

Rédacteur en chef suppléant
S. KULCZYŃSKI

CLASSE TROISIÈME

Rédacteur de la Série
L. INFELD

Comité de Rédaction de la Série
K. BORSUK, S. LESZCZYCKI, J. SAMSONOWICZ, M. ŚMIAŁOWSKI

VOLUME I
NUMÉROS 3—4

VARSOVIE 1953

PRINTED IN POLAND

PAŃSTWOWE WYDAWNICTWO NAUKOWE — WARSZAWA 1953

Nakład 1150 egz. + 50 odb.	Rękopis dostarczono 30. IV. 1953
Ark. wyd. 5·2, druk. 5·5	Podpisano do druku 17. VIII. 1953
Papier bezdrzewny sat. 70 g, III kl.	Druk ukończono 29. VIII. 1953
Format 70×100 cm/16	Zam. prod. 220/53 Cena zł 10·—

KRAKOWSKA DRUKARNIA NAUKOWA, KRAKÓW, UL. CZAPSKICH 4

BULLETIN DE L'ACADÉMIE
POLONAISE DES SCIENCES
Cl. III — Vol. I, Nos 3—4, 1953

MATHÉMATIQUE

Sur une relation entre la façon de la mise en équation du problème physique et la notion des solutions généralisées des équations aux dérivées partielles du second ordre

par

T. WAŻEWSKI

Présenté à la séance du 20 Octobre 1952

I. Désignons par C une corde matérielle rectiligne, homogène, infiniment mince, parfaitement élastique dont le coefficient d'élasticité $e = 1$ et dont la densité linéaire à l'état naturel $r = 1$.

La distance s (dotée d'un signe convenable) d'un point physique quelconque P de C (à l'état naturel) à un point physique fixe A constitue sa coordonnée lagrangienne attachée invariablement à P pendant le mouvement éventuel de C. En admettant l'absence de forces extérieures, supposons que C vibre longitudinalement en restant au cours du mouvement sur un axe immobile x. La position du point s (c.-à-d. du point physique à coordonnée lagrangienne s) à l'instant t sera indiquée par une équation de la forme $x = u(t, s)$. Soit $M(a, b)$ un segment de C déterminé par l'inégalité $a \leqslant s \leqslant b$ $(a < b)$.

II. Voici d'abord la première façon F_1 de mettre en équation le mouvement de C. Elle consistera à adopter les hypothèses suivantes:

H_1) $u(t, s)$ est de classe C_1, c.-à-d. qu'elle possède les dérivées partielles continues du premier ordre.

H_2) La masse de $M(a, b)$ est constante au cours du mouvement.

H_3) L'accélération du centre de masse de $M(a, b)$ multipliée par la masse de $M(a, b)$ est égale à la somme vectorielle des tensions élastiques exercées sur $M(a, b)$ aux points a et b. Cette hypothèse indique que

$$\text{(J)} \qquad \frac{d^2}{dt^2}\int_a^b u(t, s)\,ds = u_s(t, b) - u_s(t, a)$$

(J) représente une famille d'équations intégro-différentielles dépendant de deux paramètres arbitraires a et b. La relation (J) doit être vérifiée pour tous les t, a et b. Cette façon de la mise en équation conduit au théorème suivant:

III. Théorème 1. *Dans les hypothèses H_1, H_2, H_3 la solution générale de* (J) *envisagée dans le voisinage d'un point quelconque (t_0, s_0) a la forme*

$$u(t, s) = f(s+t) + g(s-t) \tag{1}$$

où $f(z)$ et $g(z)$ sont de classe C_1 respectivement au voisinage du point $z = s_0 + t_0$ et $z = s_0 - t_0$.

La démonstration s'appuie sur l'équivalence de la relation (J) à l'équation

$$\int_a^b [u_t(q, s) - u_t(p, s)]ds = \int_p^q [u_s(t, b) - u_s(t, a)]dt \tag{J bis}$$

où a, b, p, q sont arbitraires. Considérons l'intégrale curviligne:

$$w(B) = \int_B [u_t(t, s)ds + u_s(t, s)dt] \tag{2}$$

prise le long du contour fermé B. Or (J bis) exprime que $w(B) = 0$ lorsque B constitue le périmètre du rectangle $a \leqslant s \leqslant b$, $p \leqslant t \leqslant q$ ou d'un polygone quelconque présentant une somme de rectangles de cette sorte. En appliquant une approximation convenable on démontre que $w(B)$ est nul pour un polygone B tout à fait général. La rotation du système de coordonnées t, s d'un angle $\frac{\pi}{4}$ conduit à un système de coordonnées m, n. La fonction $u(t, s)$ rapportée à ce système prendra la forme $v(m, n)$. La relation $w(B) = 0$ prendra la forme $P - Q = 0$ où

$$P = \int_B v_m(m, n)dm, \qquad Q = \int_B v_n(m, n)dn.$$

Comme il est évident que $P + Q = 0$, il en résulte que P et Q sont nuls pour tout polygone B. Soit maintenant B un rectangle $c \leqslant m \leqslant h$, $d \leqslant n \leqslant k$. En différentiant P par rapport à h on prouve que $v_m(m, n)$ ne dépend pas de n. On prouve de même que $v_n(m, n)$ ne dépend pas de m. Il en résulte que $v(m, n)$ a la forme $F(m) + G(n)$, d'où résulte la relation (1)*).

IV. Supposons que les valeurs de $u(t, s)$ soient données à l'instant $t = 0$ pour $0 \leqslant s \leqslant 1$ ainsi que sur les lignes $s = 0$ et $s = 1$ pour tous les t, ces fonctions données étant de classe C_1. La dérivée $u_t(t, s)$ soit égale à une fonction continue donnée pour $t = 0$. En appliquant un raisonnement analogue au raisonnement classique (où $u(t, s)$ est de classe C_2) et en s'appuyant sur le Théorème 1 on prouvera que ce problème mixte relatif à (J) admet une solution unique de classe C_1 qui dépend d'une façon continue des valeurs initiales et latérales de $u(t, s)$. Ce problème est donc correctement posé au sens de Hadamard relativement à la famille des fonctions de classe C_1.

*) Une démonstration de ce théorème basée sur un autre principe a été indiquée par A. Pliś.

V. Soit $f(z)$ une fonction dont la première dérivée est continue partout et dont la seconde dérivée n'existe nulle part (Weierstrass). La fonction $u(t, s) = f(s + t)$ vérifiera évidemment (J) pour tous les a, b, t. L'accélération du centre de masse de chaque segment $M(a, b)$ existera donc à chaque instant t. D'autre part, l'accélération $u_{tt}(t, s)$ n'existera à aucun instant pour aucun point physique s.

VI. Passons maintenant à une autre façon F_2 de la mise en équation du mouvement de C en complétant les hypothèses H_1, H_2, H_3 par la suivante:

Hypothèse H_4. La dérivée continue $u_{tt}(t, s)$ existe pour tout t et s. Il en résulte que chaque point physique possède une accélération déterminée.

On voit facilement que, dans les hypothèses $H_1 - H_4$, l'équation (J) est équivalente à l'équation classique

(D) $$u_{tt}(t, s) = u_{ss}(t, s).$$

La première mise en équation conduit à l'équation (J bis) dans laquelle n'interviennent que les premières dérivées, tandis que la deuxième mise en équation conduit à l'équation (D) à dérivées partielles du second ordre. Chaque solution de (D) est une solution de (J). L'inverse n'étant pas juste, (D) et (J) ne sont pas équivalentes. Dans la théorie du mouvement des milieux continus plus généraux on peut appliquer les façons de la mise en équation analogues à F_1 et F_2 qui conduisent aux équations intégro-différentielles d'une part et différentielles d'autre part qui, en général, ne sont pas équivalentes.

VII. S. L. Sobolev ([1], page 307) a introduit la notion des solutions généralisées G des équations du type hyperbolique qui constituent les limites (en un certain sens) des solutions (au sens classique) G_n d'un problème mixte d'une suite d'équations différentielles. Notre théorème implique que les solutions de classe C_1 de (J) qui ne satisfont pas à (D) constituent des solutions généralisées de (D) au sens de S. L. Sobolev. Il est, peut-être, intéressant que la mise en equation F_1 attache une certaine interprétation physique à une classe de solutions généralisées au sens de S. L. Sobolev.

VIII. La notion du milieu matériel continu englobant celle du point physique constitue une simplification qui fait abstraction de la structure atomique de la matière. D'autre part le problème mixte pour la corde C relatif à la façon F_1 est bien posé même sans l'hypothèse H_4. Ceci nous amène à la question si l'hypothèse H_4 (adoptée sous différentes formes dans la plupart des cours de Mécanique) est nécessaire pour arriver aux conséquences de caractère physique conformes à l'expérience. Si l'on réussissait à établir qu'il n'en est pas ainsi, H_4 apparaîtrait comme une hypothèse de caractère mathématique (et non pas physique) faisant perdre une classe de solutions correspondant à F_1 qui ne sont pas de classe C_2.

Les considérations de la présente note ne donnent évidemment pas de raisons suffisantes pour trancher cette question bien délicate. Une remarque

de I. G. Petrovsky (cf. [2], p. 84) est, dans une certaine mesure, liée à ce problème.

IX. Il serait peut-être intéressant d'examiner le problème mixte correspondant à la façon F_1 pour les milieux matériels continus plus généraux que la corde C, en admettant aussi des forces extérieures. L'esquisse de la démonstration du Théorème 1 fait entrevoir les difficultés liées avec l'examen des équations intégro-différentielles analogues à l'équation (J).

BIBLIOGRAPHIE

[1] Sobolev S. L., *Urawnienia matematiczeskoj fiziki.*

[2] Petrovsky I. G., *Lekcii ob urawnieniach s czastnymi proizwodnymi.*

BULLETIN DE L'ACADÉMIE
POLONAISE DES SCIENCES
Cl. III — Vol. I, Nos 3—4, 1953

MATHÉMATIQUE

Une application géométrique du théorème de Brouwer sur les points invariants

par
K. KURATOWSKI et H. STEINHAUS

Présenté à la séance du 23 Février 1953

Imaginons, sur le plan euclidien, une région bornée R (ou, plus généralement, un ensemble mesurable borné). Soit $\varrho = |R|$ l'aire de l'ensemble R. Désignons par A_0, A_1 et A_2 les angles déterminés par trois rayons issus du même point (voir Fig. 1), et par A le triple qui les détermine.

Soient, enfin, α_0, α_1 et α_2 trois nombres tels que

$$\alpha_0 + \alpha_1 + \alpha_2 = 1, \qquad \alpha_i \geqslant 0 \quad \text{pour } i = 0, 1, 2.$$

Nous affirmons qu'en effectuant une translation convenable de l'ensemble A, cet ensemble (ainsi transféré) partage l'ensemble R en trois parties de façon que la partie de l'ensemble R contenue dans l'angle A_i ait l'aire $\varrho\alpha_i$ pour $i = 0, 1, 2$ (voir Fig. 2).

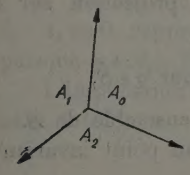

Fig. 1

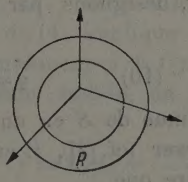

Fig. 2

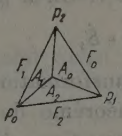

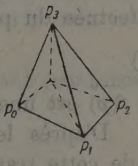

Fig. 3

On obtient évidemment un énoncé équivalent en supposant que l'ensemble A reste fixe, tandis que l'ensemble R est soumis à une translation. C'est bien cet énoncé que nous allons établir (au N III); de plus, nous allons le généraliser à l'espace n-dimensionnel.

I. Notations. Rappelons qu'étant donné dans l'espace euclidien $\mathcal{E}^n$ à n dimensions un système de $n+1$ points $p_0, \ldots, p_n$ linéairement indépendants, on appelle simplexe (fermé) $S = p_0 \ldots p_n$ l'ensemble des points p de la forme

(en notation vectorielle)

(1) $$p = \lambda_0 p_0 + \ldots + \lambda_n p_n, \text{ où } \lambda_0 + \ldots + \lambda_n = 1 \text{ et } \lambda_i \geqslant 0.$$

Nous désignons par F_i la *face* du simplexe opposée au sommet p_i; c'est donc l'ensemble des points p de la forme (1), où $\lambda_i = 0$.

$\dot{S}$ désigne le *bord* du simplexe S. Il vient

(2) $$\dot{S} = F_0 + \ldots + F_n, \qquad (3) \qquad F_0 \cdot \ldots \cdot F_n = 0.$$

Nous admettons (ce qui n'est d'ailleurs nullement essentiel) que le point 0 est un point intérieur du simplexe S et nous désignons par A_i *l'angle* composé de tous les points de la forme βp, où $p \in F_i$ et où $\beta \geqslant 0$ (cf. Fig. 3). On a donc

(4) $$F_i = \dot{S} A_i, \qquad (5) \qquad \mathcal{E}^n = A_0 + \ldots + A_n.$$

Il résulte de (3) et (4) que

(6) $$\dot{S} \cdot A_0 \cdot \ldots \cdot A_n = 0,$$

d'où on conclut facilement (voir par exemple [1], p. 15) qu'il existe un nombre $\eta > 0$ (nommé coefficient correspondant au système $\dot{S}, A_0, \ldots, A_n$) jouissant de la propriété suivante:

(7) pour tout ensemble R les conditions $\dot{S}R \neq 0$ et $\delta(R) < \eta$*) entraînent $RA_i = 0$ pour au moins un indice i.

II. Lemme topologique. *Soit f une transformation continue du simplexe S en un sous-ensemble de S. Dans l'hypothèse que*

(8) $$p \in \dot{S} \quad \textit{implique} \quad p \neq f(p) \in \dot{S},$$

on a $f(S) = S$, c'est-à-dire que tout point de S est une valeur de la fonction f.

Démonstration. Supposons par contre que $S - f(S) \neq 0$. L'ensemble $f(S)$ étant fermé, il existe donc un point intérieur r de S qui n'appartient pas à $f(S)$. Pour tout point $q \neq r$, désignons par $\vec{q}$ sa projection sur $\dot{S}$ effectuée du point r. On a donc

(9) $$\vec{q} \in \dot{S}, \qquad (10) \qquad \vec{q} = q \text{ pour } q \in \dot{S},$$

et $\vec{f}(p)$ est une transformation continue de S en un sous-ensemble de S.

D'après le théorème de Brouwer (cf. [2]), il existe un point invariant p de cette transformation, c'est-à-dire que

(11) $$\vec{f}(p) = p.$$

Donc, d'après (9), $p \in \dot{S}$ et selon (8)

(12) $$p \neq f(p) \in \dot{S},$$

d'où $\vec{f}(p) = f(p)$ en raison de (10).

*) $\delta(R)$ est la borne supérieure des distances mutuelles des points de R.

Mais alors $p = f(p)$ en vertu de (11), ce qui est incompatible avec (12). Cette contradiction prouve que $f(S) = S$.

III. Théorème. *Soit, dans l'espace euclidien $\mathcal{E}^n$, à n dimensions, R_0 un ensemble borné contenant le point 0. Soit R_p l'ensemble qui s'obtient de R_0 par la translation $p + x$.*

*Admettons (en nous servant des notations du NI) que $\delta(R_0) < \eta$ *).*

Soit $|R_0| = \varrho$ (mesure n-dimensionnelle de l'ensemble R_0).

Admettons enfin que les nombres $\alpha_0, \ldots, \alpha_n$ satisfont aux conditions

$$\alpha_0 + \ldots + \alpha_n = 1, \qquad \alpha_i \geqslant 0 \quad \text{pour} \quad i = 0, \ldots, n. \tag{13}$$

Il existe alors un point $p \in S$ tel que

$$|R_p \cdot A_i| = \varrho \alpha_i \qquad \text{pour} \quad i = 0, \ldots, n. \tag{14}$$

Démonstration. Posons

$$\lambda_i(p) = \frac{1}{\varrho} |R_p \cdot A_i|. \tag{15}$$

Donc $\lambda_i(p) \geqslant 0$ et — comme $|A_i \cdot A_j| = 0$ pour $i \neq j$ —

$$\lambda_0(p) + \ldots + \lambda_n(p) = \frac{1}{\varrho} |R_p \cdot (A_0 + \ldots + A_n)| = \frac{1}{\varrho} |R_p| = 1,$$

d'après (5) et d'après l'égalité $|R_p| = \varrho$.

Les nombres $\lambda_0(p), \ldots, \lambda_n(p)$ peuvent donc être considérés comme coordonnées barycentriques d'un point — désignons le par $f(p)$ — du simplexe S:

$$f(p) = \lambda_0(p) \cdot p_0 + \ldots + \lambda_n(p) \cdot p_n. \tag{16}$$

D'après (15) la fonction f est continue. Nous allons démontrer qu'elle satisfait à la condition (8).

Soit, en effet, $p \in \dot{S}$. Comme $p \in R_p$, nous avons $\dot{S} R_p \neq 0$. Il existe donc d'après (7) un indice i tel que $R_p \cdot A_i = 0$, d'où $|R_p \cdot A_i| = 0$, donc $\lambda_i(p) = 0$. Il en résulte que $f(p) \in F_i$, donc $f(p) \in \dot{S}$. En même temps, la formule $R_p \cdot A_i = 0$, rapprochée de (4), implique que $R_p \cdot F_i = 0$, donc p non-$\in F_i$ (puisque $p \in R_p$). Par conséquent $p \neq f(p)$.

L'implication (8) étant établie, on en conclut qu'en posant (conformément à (13))

$$r = \alpha_0 p_0 + \ldots + \alpha_n p_n, \tag{17}$$

il existe un point $p \in S$ tel que $f(p) = r$.

Les formules (16) et (17) impliquent que

$$\lambda_i(p) = \alpha_i \quad \text{pour} \quad i = 0, \ldots, n,$$

d'où la formule (14) en vertu de (15).

---

*) Cela peut être admis sans restreindre la généralité du problème, car en remplaçant le simplexe S par un simplexe homothétique aussi grand qu'on le veut, on n'altère pas les angles $A_0, \ldots, A_n$.

IV. Généralisation. Soit $q = h(p)$ une transformation continue du simplexe S en un sous-ensemble d'un espace compact Y. Soit $A_0, \ldots, A_n$ un système d'ensembles fermés tels que

$$1^0 \quad Y = A_0 + \ldots + A_n, \qquad 2^0 \quad h(\dot{S}) \cdot A_0 \cdot \ldots \cdot A_n = 0, \qquad 3^0 \quad h(F_i) \subset A_i.$$

Soit $\eta > 0$ le coefficient correspondant au système $h(\dot{S})$, $A_0, \ldots, A_n$.

Admettons que dans l'espace Y on a défini une mesure (additive, non négative, nulle pour l'ensemble vide) et que l'on a fait correspondre à tout point q de $h(S)$ un ensemble $R_q \subset Y$ de façon que:

$$4^0 \quad q \in R_q, \qquad 5^0 \quad \delta(R_q) < \eta, \qquad 6^0 \quad |R_q| = \varrho \quad \text{(const.)},$$

$$7^0 \quad |R_q \cdot A_i \cdot A_j| = 0 \quad \text{pour } i \neq j,$$

8^0 $|R_q \cdot A_i|$ est une fonction continue de q.

Dans ces hypothèses, à tout système $\alpha_0, \ldots, \alpha_n$ satisfaisant aux conditions (13), correspond un point q tel que $|R_q \cdot A_i| = \varrho \alpha_i$ pour $i = 0, \ldots, n$.

La démonstration est tout-à-fait analogue à la précédente, sauf que l'on remplace la formule (15) par

$$(15') \qquad \lambda_i(p) = \frac{1}{\varrho} |R_{h(p)} \cdot A_i| \quad \text{pour} \quad p \in S.$$

Pour une généralisation différente, voir la note qui suit de K. Borsuk.

Institut Mathématique de l'Académie Polonaise des Sciences

BIBLIOGRAPHIE

[1] Kuratowski K., *Topologie* I. Monogr. Mat. 1950.

[2] Knaster B., Kuratowski K., Mazurkiewicz S., *Ein Beweis des Fixpunktsatzes für n-dimensionale Simplexe*, Fund. Math. **14** (1929), 132.

BULLETIN DE L'ACADÉMIE
POLONAISE DES SCIENCES
Cl. III — Vol. I, Nos 3—4, 1953

MATHEMATICS

An Application of the Theorem on Antipodes to the Measure Theory

by
K. BORSUK

Communicated at the meeting of February 23, 1953.

Let Q be a n-dimensional Euclidean sphere, defined in the n-dimensional Euclidean space E^n by the inequality

$$\varrho(x, 0) \leqslant r.$$

For every point $x = (x_1, x_2, \ldots, x_n)$ lying on the boundary S of Q the point $x^* = (-x_1, -x_2, \ldots, -x_n)$ will be called the *antipode* of x. By the *theorem on antipodes* we mean the following statement [1]:

If φ is a continuous mapping of S into itself such that

$$\varphi(x^*) = [\varphi(x)]^* \qquad \text{for every } x \in S,$$

*then φ is essential**) (more exactly, the degree of φ is odd).

It is easy to observe that the theorem on antipodes can also be formulated in the following manner:

If φ is a continuous mapping of S into a set S' homeomorphic with S and if $\varphi(x) \neq \varphi(x^*)$ for every point $x \in S$ then φ is essential.

It follows that if φ maps S into the boundary $\dot{\Delta}$ of an n-dimensional simplex Δ and if $\varphi(x) \neq \varphi(x^*)$ for every $x \in S$, then for every continuous extension of mapping φ onto Q, with values on Δ, we have $\varphi(Q) = \Delta$.

The aim of this note is to apply the theorem on antipodes to prove a theorem concerning measure, which makes it possible to obtain a short proof of a theorem by K. Kuratowski and H. Steinhaus.

Let M be a metric space and $\mathfrak{M}$ a field of subsets of M (called *measurable sets*) in which an additive and not negative function (measure) is defined. The measure of a set $A \in \mathfrak{M}$ will be designed by $|A|$.

Let $M_0, M_1, \ldots, M_k$ be a finite system of subsets M. By $\alpha(M_0, M_1, \ldots, M_k)$ we denote the upper bound of the set composed of all numbers α such

---

*) A continuous mapping of a space X into a space Y is said to be *essential*, if it is not homotopic to a constant mapping.

that the relations

$$A \subset M \quad \text{and} \quad A \cdot M_i \neq 0 \quad \text{for every } i = 0,1,\ldots,k$$

imply that the diameter $\delta(A)$ of A is $\geqslant a$. Evidently $a(M_0, M_1, \ldots, M_k)$ is finite if and only if each of the sets $M_0, M_1, \ldots, M_k$ is not empty, and it is positive, if $M_0, M_1, \ldots, M_k$ are compact and $M_0 \cdot M_1 \cdot \ldots \cdot M_k = 0$.

Theorem. *Let $M = M_0 + M_1 + \ldots + M_k$ $(k \leqslant n)$ be a decomposition of the space M into $k+1$ sets M_i and let f be a continuous mapping of the sphere Q into M. Moreover, for every $p \in f(Q)$, let A_p denote a measurable set such that:*

1^0 $0 < |A| < \infty$ for *every* $p \in f(Q)$,

2^0 *$A_p \cdot M_i$ is measurable and $|A_p \cdot M_i|$ depends continuously on the point $p \in f(Q)$, for every $i = 0,1,\ldots,k$,*

3^0 $|A_p \cdot M_i \cdot M_j| = 0$ *for every $p \in f(Q)$ and $i \neq j$.*

If $k < n$ then

(I) There exist two antipodal points $x, x^* \in S$ such that the numbers $|A_{f(x)} \cdot M_0|, |A_{f(x)} \cdot M_1|, \ldots, |A_{f(x)} \cdot M_k|$ are proportional to the numbers $|A_{f(x^*)} \cdot M_0|, |A_{f(x^*)} \cdot M_1|, \ldots, |A_{f(x^*)} \cdot M_k|$.

If, however $k = n$ and

4^0 *$\delta(A_p) < a(M_0, M_1, \ldots, M_n, f(S))$ and $A_p \cdot f(S) \neq 0$ for every $p \in f(S)$ then either (I) holds or*

(II) For every system $\gamma_0, \gamma_1, \ldots, \gamma_n$ of positive numbers there exists a point $x \in Q - S$ such that the numbers $|A_{f(x)} \cdot M_0|, |A_{f(x)} \cdot M_1|, \ldots, |A_{f(x)} \cdot M_n|$ are proportional to the numbers $\gamma_0, \gamma_1, \ldots, \gamma_n$.

Proof. Setting

$$\lambda_i(x) = \frac{|A_{f(x)} \cdot M_i|}{|A_{f(x)}|} \quad \text{for every } x \in Q \text{ and } i = 0,1,\ldots,k, \tag{1}$$

we obtain (by 1^0, 2^0 and 3^0) a system of continuous, non-negative functions $\lambda_0, \lambda_1, \ldots, \lambda_k$ such that

$$\lambda_0(x) + \lambda_1(x) + \ldots + \lambda_k(x) = 1 \quad \text{for every } x \in Q.$$

Consider now a k-dimensional simplex Δ with vertices $a_0, a_1, \ldots, a_k \in E^n$. Setting

$$\varphi(x) = \sum_{i=0}^{k} \lambda_i(x) \cdot a_i \quad \text{for every } x \in Q, \tag{2}$$

we obtain a continuous mapping φ of Q into Δ. If $k < n$ then we infer, by the theorem on antipodes, that there exists a point $x \in S$ such that $\varphi(x) = \varphi(x^*)$. Consequently we have $\lambda_i(x) = \lambda_i(x^*)$ for every $i = 0,1,\ldots,k$, i. e. (I) holds.

If, however, $k = n$ and the condition 4^0 is satisfied, then there exists, for every point $x \in S$, an index i_x such that $A_{f(x)} \cdot M_{i_x} = 0$ and consequently $\lambda_{i_x}(x) = 0$. It follows that φ maps S into the boundary $\dot{\Delta}$ of Δ. Now let us assume that (I) does not hold. Hence for every $x \in S$ the points $\varphi(x)$

and $\varphi(x^*)$ are different. As we have already observed, it follows, by the theorem on antipodes, that the mapping φ is essential on S and consequently $\varphi(Q) = \Delta$. We infer that there exists a point $x \in Q - S$ such that

$$\varphi(x) = \gamma_0 \cdot a_0 + \gamma_1 \cdot a_1 + \ldots + \gamma_n \cdot a_n,$$

i. e. $\lambda_i(x) = \gamma_i$ for every $i = 0,1,\ldots,k$. It follows by (1) that the numbers $|A_{f(x)} \cdot M_i|$ are proportional to the numbers γ_i, i. e. (II) holds. This completes the proof of the theorem.

Let us show that our theorem involves the following theorem due to K. Kuratowski and H. Steinhaus *).

Let 0 *be an interior point of an n-dimensional simplex*

$$\Delta = (a_0, a_1, \ldots, a_n) \subset E^n$$

and let M_i *denote the sum of all rays starting from* 0 *and meeting the* $(n-1)$*-dimensional face* $(a_0, a_1, \ldots, a_{i-1}, a_{i+1}, \ldots, a_n)$ *of* Δ. *For every measurable (in the sense of Lebesgue), bounded subset* A *of* E^n *and every system* $\gamma_0, \gamma_1, \ldots, \gamma_n$ *of positive numbers with* $\gamma_0 + \gamma_1 + \ldots + \gamma_n = 1$ *there exists a translation* ϑ *mapping* A *onto a set* $\vartheta(A)$ *such that*

$$|\vartheta(A) \cdot M_i| = \gamma_i \cdot |A| \qquad \text{for every } i = 0,1,\ldots,n. \tag{3}$$

Proof. Since the case in which $|A| = 0$ is trivial, we can assume that $|A| > 0$. Moreover we can assume that the point 0 belongs to A. Let us denote by A_p, for every point $p \in E^n$, the set obtained from A by the translation

$$\vartheta(x) = p + x. \tag{4}$$

As before, we denote by Q the sphere in E^n with center 0, radius r and boundary S. It is evident that for r sufficiently large we have

$$\delta(A) < \alpha(M_0, M_1, \ldots, M_n, S).$$

Since no one of the closed sets M_i contains two antipodal points of S, we can easily see that for r sufficiently large: for every $p \in S$ and $i = 0,1,\ldots,n$ at least one of sets $A_p \cdot M_i$ and $A_{p^*} \cdot M_i$ is empty.

Evidently, for every $p \in E^n$ it is

$$|A_p| = \sum_{i=0}^{n} |A_p \cdot M_i|. \tag{5}$$

Since $|A_p| = |A| > 0$, there exists, for every $p \in S$, an index i_p such that $|A_p \cdot M_{i_p}| > 0$.

Now we apply our theorem, putting $M = E^n$ and $f =$ the identical mapping. Then the conditions $1^0 - 4^0$ are satisfied. Moreover we have

$$\lambda_{i_p}(p) = \frac{|A_p \cdot M_{i_p}|}{|A_p|} \neq 0 \quad \text{and} \quad \lambda_{i_p}(p^*) = \frac{|A_{p^*} \cdot M_{i_p}|}{|A_p|} = 0.$$

*) See the previous communication.

Consequently (I) does not hold. It follows that (II) holds, i. e. there exists a point $p \in Q - S$ such that the numbers $|A_p \cdot M_0|, |A_p \cdot M_1|, \ldots, |A_p \cdot M_n|$ are proportional to the numbers $\gamma_0, \gamma_1, \ldots, \gamma_n$. It follows, by (5), that the coefficient of proportionality is equal to $|A_p| = |A|$. It means that the translation ϑ, defined by formula (4) satisfies condition (3), i. e. the proof of the theorem of Kuratowski and Steinhaus is finished.

REFERENCES

[1] Borsuk K., *Drei Sätze über die n-dimensionale euklidische Sphäre*, Fund. Math. **20** (1933), 177—190.

BULLETIN DE L'ACADÉMIE
POLONAISE DES SCIENCES
Cl. III — Vol. I, Nos 3—4, 1953

MATHEMATICS

Concerning the Cartesian Division by Manifold

by

K. BORSUK

Communicated at the meeting of February 23, 1953.

1. A space Z is said to be *divisible* by a space Y if there exists a space X such that Z is homeomorphic with the Cartesian product $X \times Y$. Then we shall refer X as the *result* of the Cartesian division of Z by Y. It is known [1] that in general the topological structure of X is not uniquely determined by the topological structure of Y and Z.

The purpose of this note is to show that the topological uniqueness of the Cartesian division is assured if Z is a locally connected continuum of dimension $n+1$ and Y is an n-dimensional manifold (closed or with a boundary).

2. Let X be an arbitrary space. A point $x \in X$ is said to be *Euclidean* if there exists a neighbourhood U of x in X, homeomorphic with a Euclidean space E^m (of an arbitrary dimension m). We denote by $\alpha(X)$ the set consisting of all Euclidean points of X. The components of $\alpha(X)$ will be said to be *Euclidean components* of X.

A point $x \in X$ is said to be *semi-Euclidean* if it is not Euclidean, but there exists a neighbourhood U of x in X, homeomorphic to a Euclidean closed half-space (of arbitrary dimension). By $\beta(X)$ we denote the set consisting of all semi-Euclidean points of X, and by $\gamma(X)$ — the set $X - \alpha(X) - \beta(X)$.

3. Let A be a Euclidean component of a locally connected curve C. We shall say:

1. A is of the *first type* if $\bar{A} \cdot [\beta(C) + \gamma(C)] = 0$ (i. e., if $C = A$ is a simple closed curve).

2. A is of the *second type* if $\bar{A} \cdot \beta(C) = 0$ and $\bar{A} \cdot \gamma(C)$ contains exactly one point (i. e., if $\bar{A} \neq A$ and A is a simple closed curve).

3. A is of the *third type* if $\bar{A} \cdot \beta(C) = 0$ and $\bar{A} \cdot \gamma(C)$ contains exactly two points.

4. A is of the *fourth type* if $\bar{A} \cdot \beta(C) \neq 0$.

4. Two points $x_1, x_2 \in X$ are said to be *isotopic* in X if there exists a continuous mapping $f(x,t)$ of the Cartesian product $X \times \langle 0,1\rangle$ into X, such that:

1. $f(x,0) = x$ for every $x \in X$.

2. For every $t_0 \in \langle 0,1\rangle$ the transformation $f(x,t_0)$ maps X onto itself topologically.

3. $f(x_1,1) = x_2$.

All points isotopic in X with a point $x_1 \in X$ constitute an arcwise connected subset of X called an *isotopy component* of X.

The following lemma holds:

Lemma. Let C be a locally connected curve and M a manifold (closed or with boundary). Every isotopy component of $C \times M$ has one of the following eight forms:

1. $A \times \alpha(M)$, where A is a Euclidean component of C of the first type.

2. $A \times \alpha(M)$, where A is a Euclidean component of C of the second type.

3. $A \times \alpha(M)$, where A is a Euclidean component of C of the third type.

4. $A \times \alpha(M)$, where A is a Euclidean component of C of the fourth type.

5. $A \times N_\mu$, where A is a Euclidean component of C of the first, second or third type and N_μ is a component of $\beta(M)$.

6. $[\bar{A} \cdot \beta(C)] \times M + A \times \beta(M)$, where A is a Euclidean component of C of the fourth type.

7. $(x_0) \times \alpha(M)$, where $x_0 \in \gamma(C)$.

8. $(x_0) \times N_\mu$, where $x_0 \in \gamma(C)$ and N_μ is a component of $\beta(M)$.

Moreover, if a homeomorphism h maps $C \times M$ onto the Cartesian product $C' \times M$, where C' is another locally connected curve, then h maps every isotopy component K of $C \times M$ onto an isotopy component of $C' \times M$ having the same form as K.

5. Let C be a locally connected curve. For every point $(x,y) \in C \times C$ let us denote by $\nu_c(x,y)$ the number (finite or not) of the Euclidean components A of C such that the boundary of A contains only the points x, y.

The following lemma holds:

Lemma. Let C and C' be two locally connected curves. In order that a homeomorphism h, mapping $\beta(C) + \gamma(C)$ onto $\beta(C') + \gamma(C')$, be extendable to a homeomorphism of C onto C' it is necessary and sufficient that

$$\nu_c(x,y) = \nu_{c'}(h(x), h(y))$$

for all points $x, y \in \beta(C) + \gamma(C)$.

6. Theorem. *Let C and C' be two locally connected curves and M a manifold (closed or with boundary). A necessary and sufficient condition that $C \times M$ be homeomorphic with $C' \times M$ is that C be homeomorphic with C'.*

Proof. It is evident that the homeomorphism of C with C' implies the homeomorphism of $C \times M$ with $C' \times M$. Let us suppose now that $C \times M$ is homeomorphic with $C' \times M$. If $\gamma(C \times M) = 0$, then it is easy to show that C is a simple arc or a simple closed curve and the homeomorphism of C with C' follows by simple homological computation. If, however, $\gamma(C \times M) \neq 0$, then by the lemma of No **4**, there exists a one-to-one correspondence between the points $x \in \gamma(C)$ and the isotopic components of $C \times M$ of the form $(x) \times \alpha(M)$. Setting

$$\varphi(x) = (x) \times M \qquad \text{for every} \qquad x \in \gamma(C),$$

we obtain a one-to-one correspondence between the points $x \in \gamma(C)$ and the closed sets of the form $(x) \times M$.

Moreover, to every point $x \in \beta(C)$ corresponds exactly one Euclidean component A_x of C such that $x \in \bar{A}_x$. Setting

$$\varphi(x) = (x) \times M + \bar{A}_x \times \beta(M) \qquad \text{for every } x \in \beta(C),$$

we obtain a homeomorphism mapping $\beta(C) + \gamma(C)$ onto a subset of $2^{C \times M}$ *) Moreover, for every two points $x, y \in \beta(C) + \gamma(C)$ the number $\nu_c(x, y)$ is equal to the number of those Euclidean components of $C \times M_x$ for which the boundary contains both sets, $\varphi(x)$ and $\varphi(y)$, and does not contain any other of the sets $\varphi(z)$.

Let φ' denote the homeomorphism of $\beta(C') + \gamma(C')$ into $2^{C' \times M}$ analogous to φ. Then $\nu_{c'}(x', y')$ is equal to the number of Euclidean components of $C' \times M$ for which the boundary contains both sets, $\varphi'(x')$ and $\varphi'(y')$, and does not contain any other of the sets $\varphi'(z')$.

Consider now a homeomorphism h mapping $C \times M$ onto $C' \times M$. By the lemma of No. **4** h maps every isotopy component of $C \times M$ onto an isotopy component of $C' \times M$ of the same form. It follows that h maps each of the sets $\varphi(x)$, where $x \in \beta(C) + \gamma(C)$, onto a set of the form $\varphi'(x')$. Since h induces a homeomorphism of $2^{C \times M}$ onto $2^{C' \times M}$ we infer that the mapping $\varphi(x) \to \varphi'(x')$ is a topological one. It follows that setting

$$x' = \psi(x),$$

we obtain a homeomorphism ψ mapping $\beta(C) + \gamma(C)$ onto $\beta(C') + \gamma(C')$. Moreover, it is easy to see that $\nu_c(x, y) = \nu_{c'}(\psi(x), \psi(y))$ holds for every $x, y \in \beta(C) + \gamma(C)$. By the lemma of No **5** we infer that ψ can be extended to a homeomorphism of C onto C'. Hence the curves C and C' are homeomorphic.

7. Combining the theorem of No **6** with the theorem [2] stating that a connected polytope has at most one decomposition into a Cartesian product of 1-dimensional factors, we easily obtain the following

*) 2^X denotes the space consisting of all compact subsets of a metric space X with the usual metric (of Hausdorff).

Theorem. *A locally connected continuum Z has at most one decomposition into a Cartesian product $X_0 \times X_1 \times \ldots \times X_k$, where dim $X_0 = 1$ and each of the factors $X_i, i = 1,2,\ldots,k$ is either a simple arc or a simple closed curve.*

REFERENCES

[1] Whitehead J. H. C., *On the homotopy type of manifolds*, Annals of Math. **41** (1940), 825.

[2] Borsuk K., *Sur la décomposition des polyèdres en produits cartésiens*, Fund. Math. **31** (1938), 139.

BULLETIN DE L'ACADÉMIE
POLONAISE DES SCIENCES
CL. III — Vol. I, Nos 3—4, 1953

THEORETICAL PHYSICS

On Mutual Nucleon-Nucleon Interaction through Meson Fields

by
J. WERLE

Communicated by L. INFELD at the meeting of October 20, 1952

The general formalism given in the preceding note [1] can be used for solving many problems of classical mesodynamics. Classical theory is more intuitive and obvious and therefore it has often been pointed out, as a defect of the meson theory of nuclear forces, that it gives no correspondence arguments analogous to those so helpful in atomic theory. In the present note an instance is given of how, by the use of the approximation method [1], this classical treatment of the meson field and nuclear forces can be extented until in the final result we make a simple correspondence transition to the quantum theory. Thus we shall deduce the classical form for the interaction potential between two nucleons, and the operator which we get after this simple correspondence substitution is just the same as that obtained from consistent quantum mechanical considerations.

For the sake of simplicity we shall not deal at this point with couplings containing derivatives. (These will be dealt with on another occasion). All equations of classical mesodynamics can be stated thus:

$$(\Box - \mu^2)\varphi = -4\pi g \sum_{i} \omega_{(i)}(t)\,\delta(\vec{x} - \vec{\xi}_{(i)}(t)). \tag{1}$$

The sources of the field are point nucleons (denoted by the index (i)), placed at $\vec{x} = \vec{\xi}_{(i)}(t)$. The functions of time $\omega_{(i)}(t)$ depend for their form on the covariance properties of the component φ of a given meson field. In order that we may treat simultaneously many special cases, we shall not define these functions now.

The deduction of the interaction potential between two nucleons can be made by means of the method proposed by P. A. M. Dirac [2], from the conservation laws of the energy-momentum tensor $T_{\nu\lambda}$. Except at the points $\vec{x} = \vec{\xi}_{(i)}$ where the point sources are situated, our φ satisfies the

homogeneous Klein-Fock equation. Therefore if we exclude these points we can use the tensor $T_{\nu\lambda}$ corresponding to the field free of sources and we also have the simple form $T_{\nu\lambda,\lambda}=0$ of the conservation laws there. In order to calculate the equations of motion it is convenient to use the simplified threedimensional formalism given for electrodynamics by L. Infeld and P. R. Wallace [3]. In particular, we compute the equations of motion in the case of scalar and pseudoscalar meson fields. For these two fields we have the same form of the energy-momentum tensor

$$T_{\nu\lambda}=\frac{1}{4\pi}(\varphi_{,\nu}\varphi_{,\lambda}-\tfrac{1}{2}\delta_{\nu\lambda}(\varphi_{,\alpha}\varphi_{,\alpha}+\mu^2\varphi^2)). \tag{2}$$

(We usually adopt the conventions of Tensor Calculus: repetition of a Latin index denoting Cartesian coordinates means summation from 1 to 3, Greek indices run from 1 to 4, further we put: $x^4=ict$, $\varphi_{,\alpha}=\dfrac{\partial\varphi}{\partial x^\alpha}$). To simplify the calculations we adopt a coordinate system, in which the particle considered is momentarily at rest for $t=t_1$. It is $\vec{\xi}_{(1)}(t_1)=0$; $\dot{\vec{\xi}}_{(1)}(t_1)=0$. In such a coordinate system the equations of motion of the first particle in the field of the second are

$$\begin{aligned} m_1\ddot{\xi}^k_{(1)} &= -\oint_1 (T_{kl}+\psi_{k,l})n_l\,d\delta \\ 0 &= -\oint_1 (T_{kl}+\psi_{k,l})n_l\,d\delta \end{aligned} \tag{3}$$

where we integrate over any closed surface surrounding the first nucleon only. n_l denotes the unit vector normal to the surface σ. The functions ψ_λ are determined as solutions of the equations

$$\Delta\psi_\lambda=-T_{\lambda 4,4}. \tag{4}$$

Since the result of the integration does not depend on the form of the surface, we can further simplify the calculations if we integrate over a sphere with radius $r\to 0$. But, instead of using infinite expansion and counting the contributions of different orders term by term (as is done by other authors [3]), we apply the exact formula

$$\varphi=\frac{1}{2\pi}g\int\left\{\omega_{(1)}(t')\frac{e^{-r_{(1)}(t')\sqrt{\mu^2-\nu'^2}}}{r_{(1)}(t')}+\omega_{(2)}(t')\frac{e^{-r_{(2)}(t')\sqrt{\mu^2-\nu'^2}}}{r_{(2)}(t')}\right\}e^{-i\nu'(t-t')}\,d\nu'\,dt'. \tag{5}$$

With this expression, e. g. the first of the integrals in (3) takes the form

$$\oint_1\varphi_{,k}\varphi_{,l}n_l\,d\delta=\frac{1}{4\pi^2}g^2\int\left\{\oint_1\left[\sum_{i=1}^{2}\omega_{(i)}(t')\,e^{-r_{(i)}(t')\sqrt{\mu^2-\nu'^2}}(1+r_{(i)}\sqrt{\mu^2-\nu'^2})\frac{r^k_{(i)}}{r^s_{(i)}}\right]\right.$$

$$(6)\qquad \cdot\left[\sum_{i=1}^{2}\omega_{(i)}(t'')\,e^{-r_{(i)}(t'')\sqrt{\mu^2-\nu''^2}}\,(1+r_{(i)}\sqrt{\mu^2-\nu''^2})\,\frac{r^l_{(i)}}{r^3_{(i)}}\right]\frac{x^l}{r}\,d\delta\Big\}\cdot$$
$$\cdot\,e^{-i\nu'(t_1-t')-i\nu''(t_1-t'')}\,d\nu'\,d\nu''\,dt'\,dt''$$

where $r^k_{(i)}=x^k-\xi^k(t)$; $r_{(i)}=|\,r^k_{(i)}\,|$; $r=|\,x^k\,|$.

All the integrations can be carried out very simply if we remember that only these terms which, in the limes $r\to 0$, are of the form: $\frac{x^{s_1}x^{s_2}\cdots x^{s_p}}{r^{p+2}}$ with p even, give surface integrals different from zero. Thus it is easy to see that φ^2, $\dot\varphi^2$ terms can not give any contribution. (We observe that, as regards the contribution to the inner (surface) integrals, $\dot\varphi$ is equivalent to φ, because time differentiation adds only a factor $i\nu$ which does not concern space integrations). From the above it follows at once that only those terms, which contain as a factor the field $\frac{e^{-\mu r}}{r}$ of the first particle taken at the time $t=t_1$ give integrals different from zero. In particular we see that, in the interaction term, the contribution from the first particle at time t, different from t_1, vanishes because of the relations

$$\lim_{r\to 0} r^k_{(i)}=\xi^k_{(i)}(t)\neq 0 \qquad \text{for } t\neq t_1$$

$$(7)\qquad \lim_{r\to 0}\oint f(r^k_{(i)})\frac{x^l}{r}\,d\delta=f(\xi^k_{(i)})\lim_{r\to 0}\oint\frac{x^l}{r}\,d\delta=0.$$

Finally we get the equation of motion for the first particle in the form

$$(8)\qquad m_1\ddot{\vec\xi}_{(1)}=-\operatorname{grad}_{(1)}V(1\leftarrow 2)+\vec F(1\leftarrow 1)$$

and a similar equation for the second one. $V(1\leftarrow 2)$ gives us the action of the second particle upon the first one; $\vec F(1\leftarrow 1)$ denotes the selfaction of the first particle upon itself. We are not concerned with the problem of selfaction at this place and therefore we take from equation (8) solely the form of the classical interaction "potential" $V(1\leftarrow 2)$. We obtain in this way

$$(9)\qquad \begin{aligned} V(1\leftarrow 2)&=-g^2/2\pi\,\omega_{(1)}(t_1)\int\omega_{(2)}(t_2)\,\frac{e^{-r_{(i)}(t_2)\sqrt{\mu^2-\nu^2}}}{r_{(2)}(t_2)}\,e^{-i\nu(t_1-t_2)}\,d\nu\,dt_2=\\ &=-g^2\,\omega_{(1)}(t_1)\left\{\omega_{(2)}(t_2)\frac{e^{-\mu r_{12}}}{r_{12}}-\frac{1}{2\mu}\frac{d^2}{dt_2^2}\,\omega_{(2)}(t_2)\,e^{-\mu r_{12}+\cdots}\right\}_{t_2=t_1}\end{aligned}$$

$V(2\leftarrow 1)$ can be obtained by interchanging the indices 1 and 2. Generally we have $V(2\leftarrow 1)\neq V(1\leftarrow 2)$. However, if we choose the center of the mass coordinate system we can symmetrise, to some extent, the potentials V because of the relations $-\xi^k_{(1)}=\xi^k_{(2)}$; $-\dot\xi^k_{(1)}=\dot\xi^k_{(2)}$ etc.

Now the transition to quantum theory can be made by means of a simple correspondence treatment. Namely, all the classical quantities should be re-

placed by the corresponding quantum mechanical quantities and their time derivatives by the commutators with appropriate one-particle Hamiltonians. For instance, $\omega_{(i)}$ must by replaced by the corresponding Dirac matrices: $\omega_{(i)} \to \varrho_3^{(i)}$ in the case of a scalar meson field; $\omega_{(i)} \to \varrho_2^{(i)}$ in the case of a pseudoscalar field.

A justification of this correspondence treatment and comparison of the results with those obtained by means of consistent quantum methods will be given on another occasion.

We shall discuss briefly the selfaction term in (8). Its contribution to the forces acting upon the first particle depends on the form of the entire motion of the first particle. It can not be neglected for arbitrary motions. In the case of electrodynamics we know that the selfaction term has the meaning of radiation damping ($\ddot{\xi}^k$), and can be obtained if we choose the retarded solution. It vanishes for a symmetrical solution. For meson fields we get a selfaction term different from zero even for the symmetrical solution. This can be intuitively understood if we remember that the electromagnetic field escapes faster than the particle itself, whereas this, of course, is not true for meson fields, where Green's function contains waves propagating with speeds from 0 to c.

The author wishes to express his gratitude to Prof. L. Infeld for many valuable discussions.

Institute of Theoretical Physics, University of Warsaw

REFERENCES

[1] Werle J., *A New Approximation Method for the Meson Fields*, Bull. de l'Académie Polonaise des Sciences **1** (1953), 23—26.

[2] Dirac P. A. M., Proc. Roy. Soc. **167** (1938), 148.

[3] Infeld L., Wallace P. R., Phys. Rev. **57** (1940), 797.

BULLETIN DE L'ACADÉMIE
POLONAISE DES SCIENCES
Cl. III — Vol. I, Nos 3—4, 1953

THEORETICAL PHYSICS

An Electronic Cloud in a Homogeneous Electric and Magnetic Field according to Dirac's Theory

by
L. INFELD

Communicated at the meeting of October 20, 1952

We shall consider here two cases: 1. that of an electronic cloud between two parallel condensor plates, and its motion and deformation in a homogeneous electric field; 2. the motion of an electronic cloud in a homogeneous magnetic field. We shall use throughout both the approximation method and the notation employed in a previous note [1]. (All references to the equations of the previous note will be preceded here by I. Also, the same notations are used).

1. The electron cloud in a homogeneous electric field. We know that according to (I, 20):

$$1) \qquad \underset{0}{A} = k = \frac{m}{e}; \quad (c=1)$$

Now $\underset{1}{A_k}$, $\underset{2}{A_0}$ are properly normalized solutions of Maxwell's equations. Assuming that the distance between the plates of the condensor is d, and that the plate, normal to the x-axis and placed at $x = 0$, has the potential V_0, while the other plate has the potential zero, we have:

$$(2a) \qquad \underset{1}{A_1^*} = 0; \quad \underset{1}{A^*} = 0; \quad \underset{1}{A_3^*} = 0$$

$$(2b) \qquad \underset{2}{A_0^*} = \frac{V_0}{d} x - V_0, \text{ since } \underset{2}{A_{0,1}^*} = E_{\cdot} = f_{10}.$$

Finally, to find $\underset{1}{A_k}$ and $\underset{2}{A_0}$ we must use the normalization condition (I, 9);

$$(3) \qquad 2 \underset{0}{A_0} \underset{2}{A_0} - \underset{1}{A_1^2} - \underset{1}{A_2^2} - \underset{1}{A_3^2} = 0,$$

where:

$$(4) \qquad \underset{2}{A_0} = \underset{2}{A_0^*} + \underset{1}{S_{,0}}; \quad \underset{1}{A_k} = \underset{1}{A_k^*} + \underset{1}{S_{,k}}.$$

Putting

$$S = \frac{E}{e}t + W(x) \tag{5}$$

(E is an arbitrary constant)

we have:

$$e\underset{1}{S}_{,1} = e\underset{1}{A}_1 = \sqrt{2m}\left\{E - V_0\left(1 - \frac{x}{d}\right)\right\}^{1/2} \tag{6a}$$

$$e(\underset{1}{A}_0^* + \underset{1}{S}_{,0}) = e\underset{2}{A}_0 = E - V_0 e\left(1 - \frac{x}{d}\right). \tag{6b}$$

Since $e\underset{2}{A}_0$ is the kinetic energy of an electron, ($e < 0$), the total energy is positive.

We assume $\underset{1}{A}_2 = \underset{1}{A}_3 = 0$, i. e., that the velocity of the beam is directed toward the x-axis. Such an assumption is possible, at least in this approximation.

Next we calculate $\underset{4}{\lambda}$, according to (I, 21), that is:

$$(\underset{4}{\lambda}\,\underset{0}{A}_0)_{,0} + (\underset{4}{\lambda}\,\underset{1}{A}^1)_{,1} = 0. \tag{7}$$

Since $\underset{0}{A}_0 = k$, the solution of this equation is:

$$\underset{4}{\lambda} = f\left(t - \underset{0}{A}_0 \int^x \frac{dx}{\underset{1}{A}^1}, y, z\right) \cdot (\underset{1}{A}^1)^{-1}, \tag{8}$$

where f is an *arbitrary* function. What does this solution mean physically? We know from (I, 19) that

$$-\underset{4}{\lambda} k = \varrho \tag{9}$$

Thus $\underset{4}{\lambda}$ represents essentially the charge density if we ignore the constant and the sign. Let us assume now that at $t = 0$, the density ϱ has, at a certain point $x = x_{(0)}$, a certain value $\varrho(x_{(0)})$. It will have the same value at a certain moment Δt at a point $x = x_{(0)} + \Delta x$, if

$$\Delta t - \underset{0}{A}_0 \frac{\Delta x}{\underset{1}{A}^1} = 0. \tag{10}$$

Therefore:

$$\frac{\Delta x}{\Delta t} = \underset{1}{A}_1 / \underset{0}{A}_0 = \sqrt{\frac{2}{m}}\left\{E - V_0\left(1 - \frac{x}{d}\right)e\right\}^{1/2}. \tag{11}$$

We see, therefore, that the cloud moves according to Lorentz's law of motion. Although

$$f(x_{(0)}; t_0) = f(x_{(0)} + \Delta x, t_0 + \Delta t) \tag{12}$$

if $\frac{\Delta x}{\Delta t}$ satisfies (11), we see from (8) that

$$\varrho \sim \frac{f}{v}. \tag{13}$$

Thus as v increases the density of the cloud decreases, that is, the cloud spreads out. But $\varrho v \sim f$, that is the current density remains constant at these two world points.

The next step is to calculate $\underset{2}{A}{}^*_k$ according to (I, 14). Since the equation for this is

$$\underset{3}{A}{}^*_{k,ss} - \underset{3}{A}{}^*_{s,sk} = 0, \tag{14}$$

it is consistent with these equations to put

$$\underset{3}{A}{}^*_k = 0, \tag{15}$$

Therefore the magnetic field created by the cloud will make its appearance for the first time in the fifth approximation, since λ starts with $\underset{4}{\lambda}$.

Finally, for $\underset{4}{A}_0$ we have, according to (I, 15),

$$\underset{4}{A}_{0,ss} = \underset{4}{\lambda}\,\underset{0}{A}_0 = \frac{f}{\underset{1}{A}{}^1}\,k = \underset{4}{\varrho}. \tag{16}$$

This equation represents Coulomb's law which appears in the fourth approximation. Therefore the approximation procedure can be used only if the cloud density is not too great. We see that

$e\underset{0}{A}_0$ is of the order zero,

$e\underset{1}{A}_k$ is of the order v, therefore of the order one,

$e\underset{2}{A}_k$ is of the order $\frac{1}{2}mv^2$, therefore of the order two.

Now $\underset{4}{A}_0$ is of the order $\frac{ne}{r}$, where n is the number of electrons, and r the distance from the centre of the cloud. The maximum value for $\frac{ne}{r}$ is $\frac{ne}{R}$, where R is the „radius" of the cloud. Thus $\frac{n}{R}$ must be small enough to assure the validity of the approximation method. We have:

$$\underset{4}{A}_0/\underset{0}{A}_0 \leqslant \frac{ne^2}{Rmc^2} \sim \frac{nr_0}{R}, \tag{17}$$

where r_0 is the „radius" of the electron. This means that, for the approximation method to be valid, $\frac{nr_0}{R}$ must be of the order of v^4.

There is one important point still to be made which, I believe, is the source of Dirac's difficulty and which caused him to change his original theory [2]. We do not always interpret eA_α as the momentum of the beam but only if $\varrho \neq 0$. In the case $\varrho \equiv 0$ the equation becomes a gauge invariant and the additional condition $A_\alpha A^\alpha = k^2$ has no meaning. Or, in other words, we replace Dirac's condition [3]

$$A_\alpha A^\alpha = k^2 \qquad \text{by} \tag{18}$$

$$\lambda(A_\alpha A^\alpha - k^2) = 0. \tag{19}$$

This means that the system of equations with (19) is equivalent to Dirac's equations if $\lambda \neq 0$. But if $\lambda = 0$, we have Maxwell's equations without normalization conditions.

2. An electronic cloud in a homogeneous magnetic field. A small electronic cloud has an initial velocity $\vec{v}$ in a homogeneous magnetic field in the z-direction. Thus, using a cylindrical coordinate system, we have:

$$\underset{1}{A^*_\varrho} = 0; \ \underset{1}{A^*_\varphi} = \frac{H}{2}\varrho; \ \underset{1}{A^*_z} = 0; \ \underset{2}{A^*_0} = 0, \tag{20}$$

$$H_z = H = \frac{1}{\varrho}\frac{\vartheta}{\vartheta\varrho}\,\varrho(\underset{1}{A^*_\varphi}) = \frac{1}{\varrho}\,(\varrho\,\underset{1}{A^*_\varphi})_{,\varrho}. \tag{21}$$

The normalization equation is:

$$\begin{cases} \underset{1}{A^2_\varrho} + \underset{1}{A^2_\varphi} + \underset{1}{A^2_z} = 2\,\underset{2}{A_0}\,k. \\ \underset{1}{A_\varrho} = \underset{1}{S_{,\varrho}}; \ \underset{1}{A_\varphi} = \underset{1}{A^*_\varphi} + \frac{1}{\varrho}\,\underset{1}{S_{,\varphi}}; \ \underset{1}{A_z} = \underset{1}{S_{,z}}; \ \underset{2}{A_0} = \underset{1\,1}{S_{,0}}. \end{cases} \tag{22}$$

Let us write:

$$S = \frac{E}{e}\,t + v_z\,z\,k + \beta\varphi + W(\varrho).$$

Then from (22) and

$$E = \tfrac{1}{2}\,m(v^2_{(v)} + v^2_z), \tag{23}$$

we have the following equation for $W_{,\varrho}$:

$$e^2\,W^2_{,\varrho} + \left[\frac{H}{2}\left(\varrho + \frac{\beta}{\varrho}\right)\right]^2 = m^2\,v^2_{(v)} = m^2(v^2_\varrho + v^2_\varphi), \tag{24}$$

where $v_{(v)}$ is the velocity-component in the (ϱ, φ) plane and v_z in the z direction.

The small cloud is, let us assume, at the distance R from the origin of the coordinate system. It has, as *a whole*, the velocity $v_{(v)}$ in the (ϱ, φ) plane, if the origin of the coordinate system is so chosen that

$$\beta = R^2, \tag{25}$$

since in this case we have

$$v_{\varrho,\varrho} = W_{,\varrho\varrho} = 0, \quad \text{for} \quad \varrho = R. \tag{26}$$

By the proper choice of the origin of the coordinate system at $t = 0$, we can also arrange that $W_{,\varrho} = 0$ for $\varrho = R$. This means that we choose at $t = 0$ the origin of the coordinate system in such a way that $\vec{v}_{(\tau)}$ is perpendicular to $\vec{R}$. Thus from (24) we have for $\beta = R^2$ and for $\varrho = R$

$$e^2 H^2 R^2 = m^2 v_{(\tau)}^2. \tag{27}$$

Since $(W_{,\varrho\varrho})_{\varrho=R} = 0$, the continuity equation is:

$$\left\{k \underset{4}{\lambda}_{,0} + \frac{1}{\varrho} \underset{1}{A}_{\varphi}(\underset{4}{\lambda})_{,\varphi} + (\underset{4}{\lambda})_{,z} = 0\right\}_{\varrho=R}; \quad k \underset{4}{\lambda}_{,0} + H \underset{4}{\lambda}_{,\varphi} + k \underset{4}{\lambda}_{,z} = 0. \tag{28}$$

If for $t = 0$ the function $\underset{4}{\lambda}(\varrho, \varphi, z)$ is given and vanishes quickly for $\varrho \neq R, \varphi \neq \varphi_0, z \neq z_0$, for an arbitrary moment we have

$$\underset{4}{\lambda}(\varrho, \varphi, z, t) = \lambda(\varrho, \varphi - \frac{eH}{m} t, z - v_z t), \tag{29}$$

which means that the density is constant, if

$$\begin{cases} \dot{S} = \omega = \dfrac{eH}{m} = \dfrac{H}{k} \\ \dfrac{dz}{dt} = v_z \end{cases} \tag{30}$$

The equations (27) and (30) tell us that the cloud moves according to Lorentz's law of motion.

The results obtained up to now are consistent with Lorentz's law of motion. There is, however, one case in which the results are different, viz. when $v_{(\tau)} = 0$, i. e. $R = 0$. This occurs in the case of a cloud moving in a z-direction, and must be treated separately. The origin of the coordinate system is now in the cloud and we shall assume cylindrical symmetry around the axis which passes through the origin of the coordinate system and is parallel to $\vec{H}$. The equations (20—21) are still valid. We shall solve them by taking:

$$\begin{cases} S = \dfrac{H}{4} \varrho^2 \, tg\,(\omega t) + v_z \, kz + \frac{1}{2} m \, v_z^2 \, t \\ \omega = \dfrac{H}{2k} \end{cases} \tag{31}$$

and obtain:

$$\underset{1\,1}{S}_{,0} = \underset{2}{A}_0 = \frac{H}{2} \varrho^2 \omega \cos^{-2}(\omega t); \underset{1}{A}_{\varrho} = \frac{H}{2} \varrho \, tg\,(\omega t); \underset{1}{A}_{\varrho} = \frac{H}{2} \varrho; \underset{1}{S}_{,z} = v_z k = \underset{1}{A}_z. \tag{32}$$

The next step is to calculate $\underset{4}{\lambda}$, if for $t = 0$ $\underset{4}{\lambda}(\varrho, z)$ is known. Because of axial

symmetry the continuity equation is:

$$k \underset{4}{\lambda}_{,0} \underset{1}{} + \frac{1}{\varrho} (\varrho \underset{1}{A}_{\varrho} \underset{4}{\lambda})_{,\varrho} + \underset{1}{A}_{z} \underset{4}{\lambda}_{,z} = 0, \tag{33}$$

or, putting (32) in:

$$k \underset{4}{\lambda}_{,0} + \frac{H}{2\varrho} \operatorname{tang} (\omega t) (\varrho^2 \underset{4}{\lambda})_{,\varrho} + v_z k \underset{4}{\lambda}_{,z} = 0. \tag{33a}$$

The solution of this equation is:

$$\underset{4}{\lambda}(\varrho, z, t) = \cos^2 (\omega t) \underset{4}{\lambda}(\varrho \cos \omega t, z - vt) \tag{34}$$

and the $A's$ in (32) have to be multiplied by this λ to give us the current densities. Thus from Dirac's original theory a new phenomenon follows. The cloud not only moves in a magnetic field with the velocity given to it, namely v_z, but also turns, contracts (and expands) with Larmor's frequency

Objection could be made to the equations (32) since they give infinities for $\omega t = (2n + 1) \frac{\pi}{2}$. However, one frequently meets with similar situations in an approximation procedure and this means that the approximation procedure breaks down for these critical values. But this can have no influence upon the general character of the conclusion drawn here. Do such oscillations perpendicular to the direction of the motion of the beam as a whole exist?

REFERENCES

[1] Infeld L., *On the Use of an Approximation Method in Dirac's Electrodynamics*, Bull. de l'Académie Polonaise des Sciences **1** (1953), 18—22.

[2] Dirac P. A. M., Proc. Roy. Soc. A **212** (1952), 330.

[3] Infeld L., Nature (1952), 702.

BULLETIN DE L'ACADÉMIE
POLONAISE DES SCIENCES
Cl. III — Vol. I, Nos 3—4, 1953

EXPERIMENTAL PHYSICS

Some New Nuclear Reactions Produced in Tin by Fast Neutrons

by

Z. WILHELMI, R. BRUNSZ and C. DĄBROWSKI

Communicated by A. SOŁTAN at the meeting of November 17, 1952

In the course of an investigation carried out by one of us [1] on the cross sections of (n, p) and $(n, 2n)$ reactions, the problem arose of extending them to nuclei which, on the basis of the shell structure model, might have been expected to reveal particularly low yields for these reactions. The two as yet unknown reactions

$$^{118}_{50}Sn(n, p)\,^{118}_{49}In \text{ and } ^{116}_{50}Sn(n, p)\,^{116}_{49}In$$

are of interest from the point of view of the number of protons in the nucleus of tin ($Z = 50$). The binding energy, in the nuclei of "magic" mass numbers 8, 20, 28 and 50, of the last proton have an especially high value which should show up in the low value of the cross sections assigned to reactions resulting in proton emission [2]. Our purpose is to prove the existence of the predicted reactions, and to determine their cross sections.

1. Experimental Method. On account of the small cross section which was anticipated, spectrally pure tin was used for the measurements, the impurities being not greater than 0·004 percent. The neutrons were produced by the $Li(d, n)$ reaction, the ions of heavy hydrogen having an energy of 0·75 Mev and the intensity of the beam about 160 μA. The samples of tin were irradiated together with iron samples which were placed in a position determined relatively to the tin samples. After comparing the radioactivity of tin with that of iron, and after having made some corrections we determined the ratio of cross sections of tin and iron.

The cross section of iron is known from other experimental studies [3]. The neutrons used in our experiments were not monokinetic, their spectrum extending over 14 Mev. In view of the fact that monokinetic neutrons could not be obtained, it was the mean cross section for neutrons of a given spectrum that was surveyed. This spectrum has two distinct peaks at about

13·5 Mev and 10·5 Mev and fast neutrons appear to be the most effective in this type of reaction. It appeared therefore that in our investigation we were dealing with neutrons of an energy of about 13·5 Mev and 10·5 Mev.

The radioactivity was measured by means of a G. M. counter with a mica window (3 mg/cm^2). As the isotope *In* 116, which as was anticipated would result from this reaction, is known to have a period of 13 sec, an apparatus was constructed to obtain photographic recording on a moving film. On this film the pulses of the counter, the cessation of irradiation with neutrons, the moment of placing the sample on the window, as well as the flashes for timing, were all recorded.

2. Identification of the radioactive isotopes obtained. Analysis of the decay-curve resulting from our measurements showed that, in addition to the isotopes from well-known reactions, radioactive nuclei with a period of $4.5 \pm 0{\cdot}5$ min were produced. This period is assigned to the isotope *In* 118 which has thus far been thought to be a product of the (n, p) reaction [4] only and to have a half-life identical with that of the one found by us. In addition to this, a shorter half-life was observed. It was separated by using a shorter exposure time and by cutting down the less penetrating β — radiation of the longer half-life.

As a result of these measurements the assignment of a half-life $12{\cdot}5 \pm 2$ sec for the isotope was rendered possible. From this the inference may be drawn that *In* 116, known from other reactions, and having a period of 13 sec, is present.

An additional check on this identification was made possible through measurements of the maximum energy of the β-spectrum.

The use of a filter with a surface mass of 0·53 g/cm^2, weakened the electron beam by a factor of 6. So we are led to the conclusion that the maximum energy of the β-spectrum amounts to $2{\cdot}8 \pm 0{\cdot}5$ Mev from the empirical data [5]. This agrees well with Duffield and Knight's result of 3 Mev [4].

As the heavy hydrogen which was used in the investigation might have contained some traces of light hydrogen, a check seemed desirable to ascertain whether the protons present in the beam from the reaction with *Li*, do not give a sufficiently strong radiation responsible for the isotopes examined in the (γ, p) reaction. On substituting light hydrogen for heavy, it was shown that, practically speaking, the (γ, p) reaction plays no part in forming the isotopes observed.

3. Cross section measurements. The ratio of the cross section σ for the a nucleus to the cross section, σ_b, for the b nucleus is, of course,

$$\frac{\sigma_a}{\sigma_b} = \frac{\nu_a n_b f_b k_a}{\nu_b n_a f_a k_b},$$

ν_a and ν_b giving the number of β-decays per unit time for the isotopes formed from a and b nuclei calculated for the indefinitely long time of

irradiation with neutrons and for the end of exposure; n_a and n_b being the number of a and b nuclei in the samples examined; f_a and f_b — the number of neutrons inciding on the samples a and b in unit time; k_a and k_b are coefficients correcting for the effect of the β-particle absorption by the material of which the a and b samples are composed; thus it was possible to determine the ratio of the number of the radioactive nuclei decaying in unit time in the whole sample, to the number of particles registered at the same time.

During the measurement of the cross section of *Sn* 118 the tin sample was irradiated by neutrons and then placed on the iron sample in such a manner that the tin was the nearer to the target. In order to evaluate the difference of the flux of neutrons crossing the two samples, an additional series of measurements was made, in which two identical iron samples were placed in the same position in relation to the target as previously the tin and iron samples. The ratio of the activities of the two iron samples was: f_{Fe}/f_{Sn}.

In measuring the cross section of *Sn* 116, we interchanged the tin and iron samples, so that the ratio under consideration was equal to: f_{Sn}/f_{Fe}.

In view of the small quantities of isotopes of *In* obtained, the absorption coefficient of the electrons for the isotopes of the tin samples was not determined experimentally but was computed, assuming exponential absorption of the beta radiation e. g. [8]. By simple calculation, using this assumption, the dependence of the coefficient k on the surface mass d (in g/cm^2) of the sample and on the effective mass absorption coefficient a (in cm^2/g) may be given. We have

$$k = \frac{ad}{1 - e^{ad}}$$

where a is taken from the curve drawn according to the experimental dates [5]. Similarly, k was computed for iron. The values of maximum energies in the β-spectrum were taken as follows:

for In 118,	*Em* = 1·5 Mev [4]
for In 116,	*Em* = 3 Mev [9]
for Mn 56 (*from Fe* 56),	*Em* = 0·75 Mev (20 %) *Em* = 1·04 Mev (30 %) *Em* = 2·81 Mev (50 %) [10]

In the table given below, the values obtained for ν, n, f and k are listed

Sn 118, 4·5 min	*Sn* 116, 13 sec	*Fe* 56, 2·59 hours
$\nu = 2{\cdot}51 \cdot 10^3$ min^{-1}		$8{\cdot}74 \cdot 10^5$ min^{-1}
$\nu =$	$4{\cdot}42 \cdot 10^3$ min^{-1}	$6{\cdot}21 \cdot 10^5$ min^{-1}
$n = 8{\cdot}87 \cdot 10^{20}$	$5{\cdot}20 \cdot 10^{20}$	$1{\cdot}53 \cdot 10^{22}$
$f_{Fe} : f_{Sn} = 1{\cdot}32$	0·78	
$k_{Sn} : k_{Fe} = 0{\cdot}66$	0·32	

In the computations it was not considered necessary to take into account either the effect of back scattering electron in the samples or "geometry" of the counter: the back scattering of electrons as is known from many studies [11], is not dependent on the electron energy. The tin and iron samples were placed on the window of the counter in exactly the same position; therefore the ratios of the impulses in both measurements could not have been affected either by the spectral composition or by "geometry" of the counter.

On the basis of the value of the cross section of iron, $\sigma_{Fe} = 18{\cdot}5$ mb found by Cohen, we get from the data given in the table, the following cross sections of the (n, p) reaction:

$$\sigma_{Sn\,118} = 0{\cdot}78\,\text{mb}$$
$$\sigma_{Sn\,116} = 0{\cdot}94\,\text{mb}.$$

Owing to the difficulties involved chiefly in the determination of the coefficients k, the accuracy of these values is estimated at 20 per cent.

In agreement with the predicted cross sections, those for both isotopes of tin were found much lower than the average value of cross section for (n, p) reaction thus far known. Nearly all measured cross sections for this reaction, which have been determined as yet, vary from 1 to 300 mb.

Institute for Experimental Physics, University of Warsaw

REFERENCES

[1] Wilhelmi Z., in preparation.
[2] Haxel O., Jensen J. H. D., Suess H. E.: Erg. d. Ex. Naturwiss. **26** (1952), 240.
[3] Cohen B. L., Phys. Rev. **81** (1951), 184.
[4] Duffield R. B., Knight J. D., Phys. Rev. **75** (1949), 1967.
[5] Seren L., Friedlander H. N., Turkel S. H., Phys. Rev. **72** (1947), 888.
[6] Lawson J. L., Cork J. M., Phys. Rev. **52** (1907), 531.
[7] Du Bridge L. A., cit. in Nuclear Data, National Bureau of Standards, Sept. 1950.
[8] Evans R. D., *The Science and Engineering of Nuclear Power*, Ed. Goodman, 1947.
[9] Lawson J. L., Cork J. M., Phys. Rev. **58** (1940), 580.
[10] Siegbahn K., Ark. Mat. Astr. Fys. **33a, 10**.
[11] Seliger H. H., Phys. Rev. **78** (1950), 490.

BULLETIN DE L'ACADÉMIE
POLONAISE DES SCIENCES
CL. III — Vol. I, Nos 3—4, 1953

EXPERIMENTAL PHYSICS

Effect of Thermionic Emission at Room Temperatures in Photosensitive Geiger-Müller Tubes

by

K. GROTOWSKI, A. Z. HRYNKIEWICZ and H. NIEWODNICZAŃSKI

Communicated by H. NIEWODNICZAŃSKI at the meeting of November 17, 1952

In scientific literature concerning the properties of Geiger-Müller counters some indications may be found of the existence of a temperature dependence of the background rate of G.-M. counters [1], [2]. Christoph and Haszle [1] in 1933 reported on increase of the background rate of some G,-M. counting tubes with increasing temperature. E. g., one of their counters showed an increase of the background from 30 counts per min. to 400 counts per min. when the temperature rose from 40° C to 90° C. Other investigators dealing with various temperature effects on G.-M. counting tubes give no information on temperature dependence of the background of these tubes.

In a more extensive study on the properties of photosensitive G.-M. counters, in progress of this Laboratory, a strong increase in the background of such counters with temperature increasing from 15° C to 50° C, was observed. At the same time in the case of freshly prepared and non-sensitized G.-M. counting tubes no temperature dependence could be found. These observations may explain the discrepancies reported in former papers, since it is well known [3] that G·-M. tubes, after extensive use, become photosensitive.

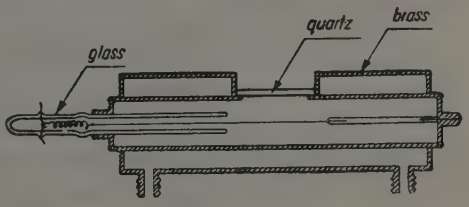

Fig. 1

In order to investigate the temperature dependence of the background of photosensitive G.-M. counters, several G.-M. tubes of a shape similar to that shown in Fig. 1 were prepared. These tubes have a double-walled brass envelope, a 0.1 mm tungsten central wire and are provided with a small quartz window. After being evacuated they were filled with the usual mixture of 90 mm Hg of argon and 10 mm Hg of dry ethyl alcohol vapour.

By circulating water from a Hoeppler ultrathermostat through the water jackets of the counters their temperature could be controlled and kept constant at any value between 15° C and 50° C.

The background counting rate of these non-sensitized tubes was found to be independent of their temperature in the temperature interval mentioned above. The figures obtained for the counting tubes *C* and *D* are given in Table I.

TABLE I

Background of non-sensitized counters

Temperature °C	Counts per min.	
	Counters	
	C	*D*
15	41	42
25	39	41
35	40	43
50	40	40

These counters were then sensitized. For this purpose they were opened, evacuated, filled with 2 mm Hg pure argon and treated by an electrical discharge (1.5 mA D. C. for 90 min.) the direction of the current being the same as in the normal functioning of G.-M. tubes. After this procedure the counting tubes became photosensitive to visible and ultraviolet light. The temperature dependence of the background of the sensitized counting tubes (with their windows covered) was investigated in the same way as it was done before the sensitizing process. A very strong increase of the background with increasing temperature was observed, as is shown in Table II for the same counting tubes *C* and *D*.

TABLE II

Background of photosensitive counters

Temperature °C	Counts per min.	
	Counters	
	C	*D*
15	67	62
20	100	87
25	171	131
30	292	206
35	533	394
40	921	711
45	1850	1306
50	2792	2232

Assuming that the increase of the background rate after sensitization is produced by thermionic emission from the sensitized brass cathode, the thermionic current for any given temperature can be determined by calculating the difference between the corresponding figures in Tables II and I If this assumption is true, the current density must obey the Richardson's equation

$$j = AT^2 e^{-\frac{\Phi}{kT}}.$$

Taking into account the fact that every electron leaving the cathode produces an impulse in the counter, the current density (in e/min. cm^2 = 2.67 · 10^{-21} A/cm^2) was calculated by dividing the number of counts per min. by the area of the effective surface of the cathode.

On the diagram in Fig. 2, log (j/T^2) is plotted against $1/T$. In the case of the counters C and D the exact linear dependence can be distinctly seen. Since, according to Richardson's formula, this regulation is represented by a straight line expressing the equation

$$\log(j/T^2) = \log A - (0.4343\,\Phi)/kT$$

our result may be considered as a proof of the pure thermionic origin of the background of the sensitized counting tubes. From the slope of the straight lines in Fig. 2 the value of the thermionic work function Φ may be obtained. E. g., for our counters C and D they are 1.03 eV and 1.01 eV respectively. The latter values relate to the electrons going out from the brass surface sensitized by electrical discharges in pure argon to the mixture of argon and alcohol vapour.

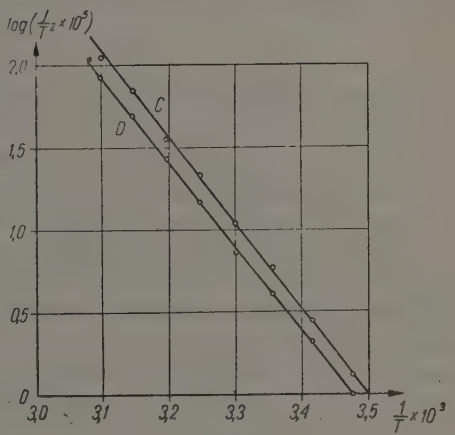

Fig. 2

Experimental verification of the validity of Richardson's equation for room temperature was made possible by the extreme sensibility of the applied method of measurement of the density of the thermionic current. In our experiments current densities of the order of 1 electron per 10 min. and per cm^2, which equals 2.7 · 10^{-22} A/cm^2, could easily be measured.

Physical Laboratory, Jagiellonian University, Cracow

REFERENCES

[1] Christoph W., Haszle W., Phys. Zeits. **34** (1933), 644.
[2] Kimura Motoharu, Phys. Rev. **80** (1950), 761.
[3] Spatz W. D. B., Phys. Rev. **64** (1943), 236.

BULLETIN DE L'ACADÉMIE
POLONAISE DES SCIENCES
Cl. III — Vol. I, Nos 3—4, 1953

EXPERIMENTAL PHYSICS

Electronic and Vibrational Energy of Tetrahydrofluorocyclene in Benzene Solution

by
Z. MAŁKOWSKI

Communicated by S. PIEŃKOWSKI at the meeting of January 12, 1953

The present work deals with the photoluminescence and absorption of tetrahydrofluorocyclene solution in benzene. The molecule which was investigated and which is a derivative of fluorocyclene belongs to a group of compounds whose structure is both peculiar and interesting. Scientific circles abroad depend for their knowledge of fluorocyclene and its derivatives on Polish sources only. The chemical properties of these compounds have been worked out by Dziewoński and his co-workers [2—7]. Optical studies on fluorocyclene and related compounds were initiated in 1932 at the Institute of Experimental Physics, University of Wàrsaw [1, 8—12, 16, 19, 20—23].

When the structural formulae of the fluorocyclene family (Fig. 1), taken from Dziewoński & Gizler's report, are compared — tetrahydrofluorocyclene, the optical properties of which have thus far not been investigated, presents the first stage in the transformation of the interior structure of the hydrocarbon with the octadiene ring coupled with the naphthylene groups (peri-tetra-naphthylene-cyclooctadiene) into the octane ring coupled with the partly hydrogenationed naphthylene groups (peri-tetra-dihydronaphthylene-cyclooctane).

The essential change in structure consisting in the gradual disappearance of coupled bonds ought to be revealed in the optical properties of the individual representatives. It is in the dodecahydrofluorocyclene that the double bonds of the central ring must disappear, and it should distinguish itself from the other hydrogenatioed derivatives of fluorocyclene by its optical properties.

Nevertheless, the expected change in the character of the spectra was not ascertained in the investigations on fluorescence and absorption of these compounds that have been thus far studied. Samples of these were kindly lent us by Prof. J. Moszew of the Institute of Organic Chemistry, Jagiellonian University, Cracow.

The optical phenomena which take place in the polyatomic molecules make it possible to investigate the transformation and transportation processes of the energy absorbed. Thus, as a result of these processes, the characteristic fluorescence and partial or complete transformation of optical energy into heat were obtained.

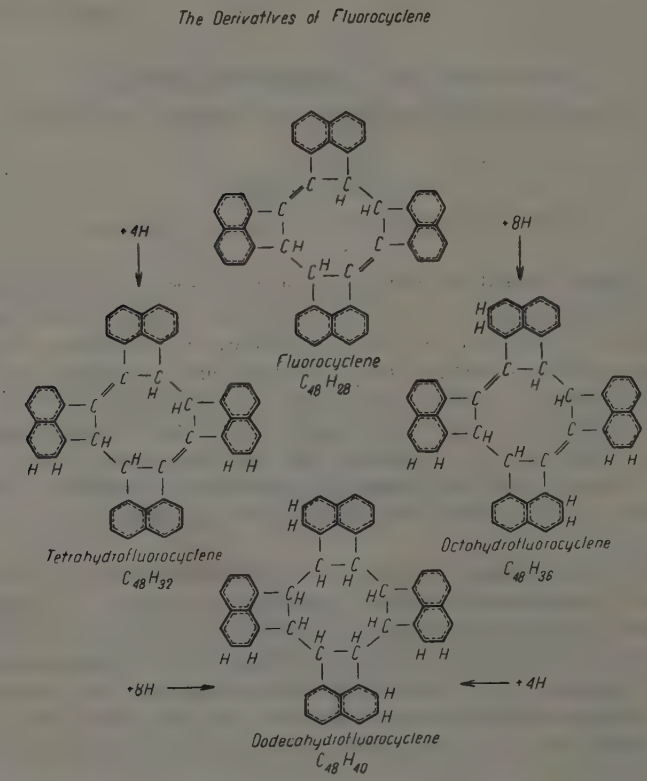

Fig. 1

The processes in the interior of the molecule depend largely upon the latter's chemical structure, hence the information gained from an investigation must either prove the correctness of the structural formulae postulated in the chemical reports, or show the necessity for some corrections.

The above-mentioned data were obtained by means of a "Unicam" photoelectric spectrophotometer and a glass Huet's C I spectrograph. In the fluorescence investigation the concentration used was of the 10^{-5} g/cm^3 order. The photometric curve of the fluorescence spectrum and the absorption

curve plotted against wave-numbers are given in Fig. 2. The absorption curve is plotted against loglog 1/T and therefore its shape depends neither upon the concentration of the solution examined, nor upon the thickness of the absorption layer (T-transmission). It may be roughly estimated from the general character of the absorption curve (A) as well as from the fluorescence curve (F), that both spectra have a vibrational structure. The po-

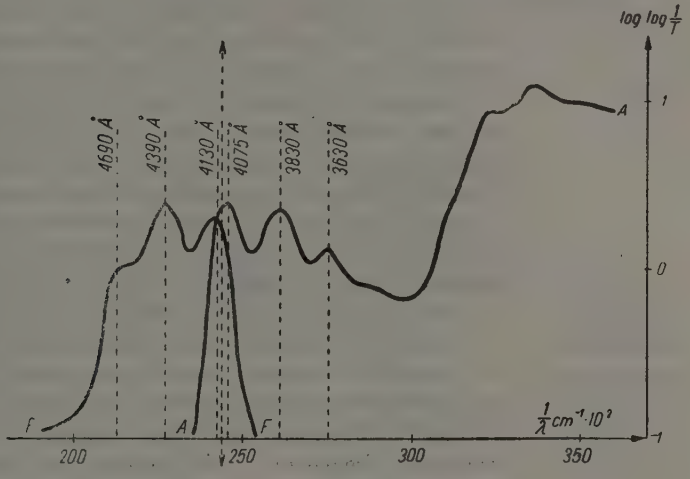

Fig. 2

sitions of the maxima for absorption and fluorescence are given in terms of wave length. On the assumption that the positions of the fluorescence band with the maximum at 4390 Å are not affected by reabsorption, an axis of symmetry for both spectra was drawn through the 24400 cm^{-1} coordinate corresponding, in terms of energy, to about 3eV. When compared, a mirror symmetry is observed in the mutual distribution along the wave-number axis of the maxima of the fluorescence and absorption bands. Reabsorption of the shortest wave-length fluorescence band causes a small shift of its maximum towards longer wave-lengths, broadening the distance between the long wave-length absorption band and the short wave-length fluorescence band. Nevertheless this distance, represented in terms of energy, is of the 0·04 eV order.

Fig. 3 shows an energy level diagram of the electronic-vibrational transitions based on the positions of the maxima for the absorption and fluorescence bands.

Nieporent has advanced the suggestion [13—17] that polyatomic molecules should be classified according to the character of their absorption and fluorescence spectra and according to whether their mutual distribution is symmetrical along the wave-number or along the wave-length axis. Thus the polyatomic molecule may be included in one of the three classes which

differ from one another in the magnitude of the coupling occurring between the molecule's own vibrations. He distinguishes simple and complex molecules, and from the latter group he excludes two subgroups in regard to the magnitude of coupling occurring between electronic and vibrational energy levels. The energetical "simplicity" of the polyatomic molecule corresponds to the high degree of symmetry in its structure.

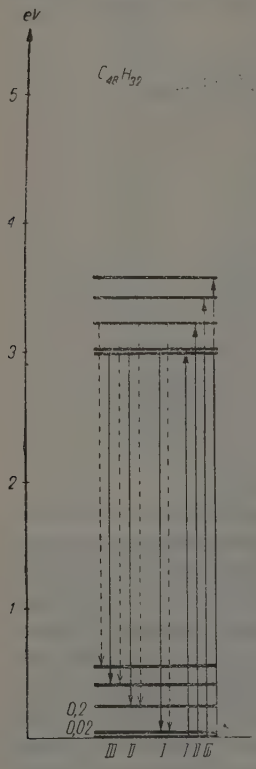

Fig. 3

The properties of absorption and fluorescence spectra which were found for the tetrahydrofluorocyclene solutions show that the molecule responsible for fluorescence should be classified in the group of the so-called simple molecules of Nieporent's classification. It seems that the carbon atoms belonging to the group constituting the central octadiene ring are the only ones responsible for the fluorescence and absorption that occur in the long wavelength region of the spectrum. The slight differences in the electronic transitions between the fundamental vibrational levels of the ground state and the excited one bear evidence to the fact that the shape of the ring in which the double bonds C = C play an essential part, undergoes only slight change. The characteristic frequency of the deformation vibrations for this group (1500 cm^{-1}) gives a specific pattern to the entire absorption and fluorescence spectrum.

As regards spectral positions and band structure, the absorption curve in the region of short wavelengths resembles closely the absorption curve for pure naphthalene solutions. Further data concerning the connection between electronic transitions and both absorption regions will be presented later.

The author wishes to express his gratitude to Professor S. Pieńkowski for suggesting this problem, his valuable help and many discussions during the course of the work. He is much obliged to the Commission for the Advancement of Science and Letters at the Council of Ministers (Komisja Popierania Twórczości Naukowej i Artystycznej przy Radzie Ministrów) for granting the scholarship which enabled him to carry on this piece of research.

Institute of Experimental Physics, University of Warsaw

REFERENCES

[1] Bednarczyk and Gizler, Bull. Ac. Pol. A (1937), 455.
[2] Doliński and Dziewoński, Bull. Ac. Pol. A (1914), 389, (1915), 44.
[3] Dziewoński and Gizler, Bull. Ac. Pol. A (1937), 441.
[4] Dziewoński and Leyko, Bull. Ac. Pol. A (1914), 287.
[5] Dziewoński and Paschalski, Bull. Ac. Pol. A (1913), 326.
[6] Dziewoński and Rapalski, Bull. Ac. Pol. A (1912), 714.
[7] Dziewoński and Suszko, Bull. Ac. Pol. A (1924), 429.
[8] Hurwicz, Ac. Phys. Pol. **1** (1932), 340.
[9] Klarner and Woszerowicz, Ac. Phys Pol. **2** (1939), 1.
[10] Małkowski, Report not yet published (1948).
[11] Makowiecka, Ac. Phys. Pol. **2** (1934), 357.
[12] Milewski, Report not yet published.
[13] Nieporent, Żurn. Fiz. Chim. **13** (1939), 965.
[14] Nieporent, Żurn. Fiz. Chim. **21** (1947), 1111.
[15] Nieporent, Żurn. Fiz. Chim. **24** (1950), 1219.
[16] Nieporent, Żurn. Eksp. i Teoret. **21** (1951), 170.
[17] Nieporent and Stiepanow, Usp. Fiz. Nauk. **43** (1951), 380.
[18] Pieńkowski, Bull. Ac. Pol. A (1937), 269.
[19] Sikorski, Report not yet published (1952).
[20] Twarowska, Ac. Phys. Pol. **2** (1933), 267.
[21] Twarowska, Ac. Phys. Pol. **4** (1935), 355.
[22] Twarowska, Bull. Ac. Pol. A (1937), 278.
[23] Twarowska, Bull. Ac. Pol. A (1938), 143.

BULLETIN DE L'ACADÉMIE
POLONAISE DES SCIENCES
Cl. III — Vol. I, Nos 3—4, 1953

EXPERIMENTAL PHYSICS

Response Time of Photoconductivity of Lead Selenide

by

L. SOSNOWSKI and M. CHMIELEWSKI

Communicated by L. SOSNOWSKI at the meeting of January 12, 1953

A method for investigating the relaxation processes in semiconductors was worked out and applied to the measurements of the response time of photoconductivity in lead selenide layers, prepared by H. Chęcińska [1].

The photoconductive layer was illuminated by means of short square-wave pulses of light. Voltage proportional to the photocurrent was applied to the vertical plates of an oscilloscope tube. The essential feature of this method consists in the use of an exponential time base i. e. the voltage on the horizontal plates keeps changing with time according to an exponential function.

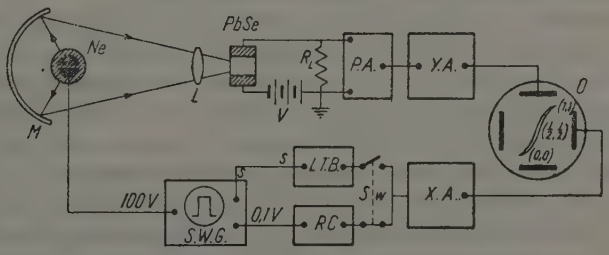

Fig. 1

A block diagram of the experimental arrangement is shown in Fig. 1. The main timing unit was a square-wave generator, which supplied 100V pulses at a rate of up to 50 000 p. s., to a neon lamp and simultaneously 0·1V pulses to the τ-meter unit. The last consisted of a decade resistance box R and fixed capacity C, which transformed the square-wave into $x = 1 - \exp(-t/RC)$ (increase) and $x = \exp(-t/RC)$ (decay). Switch Sw permitted the alternative use of an ordinary linear time base.

The light from the neon lamp was focused by a mirror M and lens system L onto a sensitive layer (cell), connected through amplifiers *P.A.*

and *Y.A.* to the vertical plates of an oscilloscope tube. *X.A.* and *Y.A.* were identical wide band amplifiers of about 60 db gain, *P.A*-about 10 db gain.

In the case of the response varying exponentially with time

$$y = 1 - \exp(-t/\tau) \qquad \text{increase}$$

and

$$y = \exp(-t/\tau) \qquad \text{decay}$$

a loop on the screen was observed. Both branches corresponding to increase and decay straightened out when $RC = \tau$. The above condition may be found with an accuracy of about 1%. When the process investigated was not exponential, a half-time T could be found, which was equal to $RC\ln 2$, when the decay (increase) curve passed through the middle point ($y = x = \frac{1}{2}$). When the decay and increase times were equal, both branches of the loop became tangent in the middle.

The above method, which has been used for Pb S by one of us (L.S.) since 1948 is in general identical with that described by Gurevitch, Tolstoy and Fieofilof [2]. The lack however of any mechanical moving parts allows measurements of times below 1 μsec to be made, which is essential in the case of lead selenide.

For such short times as these, it was necessary to keep all sources of delay due to the capacities and resistances in the generator, cell and amplifiers circuits, as small as possible. If the involved time constants are known, the shape of the loop may be calculated by means of the Laplace transformation. The shape deviates from a straight line even in the case of the pure exponential response of a photoconductive cell.

The procedure adopted was to measure the apparent response time of an emissive vacuum photocell. As the time lag of the photocell due to the transit time of the electrons was negligible, the apparent response time was due to the measuring system. The shape of the curve corresponded very well with that calculated. The response of the system may be fairly approximated by an exponential function with the parameter $\tau_0 = 0{\cdot}8\,\mu$sec.

When the emissive cell was replaced by a photoconductive cell with a response time τ, the τ-meter registered a time approximately equal to $\tau_0 + \tau$. More exactly: assuming decay of the photoconductivity according to the law $z(t) = \exp(-t/\tau)$ and time constant of the system τ_0 one finds

$$y = [\tau_0/(\tau_0 - \tau)]\exp(-t/\tau_0) + [\tau/(\tau - \tau_0)]\exp(-t/\tau)$$

as may easily be verified by the Laplace transform. Putting $x = \exp(-t/RC)$ the following equation of the decay branch of the loop is obtained:

$$y = [\tau_0/(\tau_0 - \tau)]x^{RC/\tau_0} + \tau/\tau - \tau_0)]x^{RC/\tau}.$$

From the condition: $y = 1/2$ when $x = 1/2$ the value of τ corresponding to the observed RC was found; it may differ from $RC - \tau_0$ by not more than 17%. The change in RC by 0·04 μsec corresponds to a detectable opening of the loop.

The results thus obtained for three PbSe photoconductive cells, as well as the values of their resistances and relative sensitivity are given in the following table:

Cell No	Resistance in kohms	Sensitivity (in arbitrary units)	Response time in μ sec
18	51	15	$0{\cdot}35 \pm 0{\cdot}07$
21	100	40	$0{\cdot}9 \pm 0{\cdot}1$
23	23	12	$0{\cdot}25 \pm 0{\cdot}1$

Such short times, well below 1 μsec, have not been observed so far in any other semiconductor. There seems to be a relation between response time, resistance and sensitivity, which calls for further investigation.

Institute of Experimental Physics, University of Warsaw

REFERENCES

[1] Chęcińska H., in this issue.

[2] Gurevitch, Tolstoy, Fieofilof, Journ. Exp. Theor. Phys. **20** (1950), No 9 in Russian.

BULLETIN DE L'ACADÉMIE
POLONAISE DES SCIENCES
Cl. III — Vol. I, Nos 3—4, 1953

EXPERIMENTAL PHYSICS

Photoconductive and Photovoltaic Layers of Lead Selenide

by

H. CHĘCIŃSKA

Communicated by S. PIEŃKOWSKI at the meeting of January 12, 1953

The properties of the microcrystalline layers of lead sulphide supplied an experimental basis for the barrier theory of photoelectric effects proposed by L. Sosnowski [1]. According to this theory:

1) the sensitive layer must contain n and p regions due to non-homogeneous distribution of impurity centres, both donors (lead) and acceptors (oxygen);

2) there must be a close connection between photoconductivity and photovoltaic effects due to barriers formed on boundaries of n and p regions.

The purpose of this investigation was to obtain layers of lead selenide possessing photoelectric properties analogous to those previously known to exist only in lead sulphide layers, and thus to extend the generality of the theory.

Photoconductive properties of lead selenide at low temperatures were first reported by O. Simpson [4]. There have since appeared a number of papers concerning the problem [5], [6], [7], none of which contained any data about the method of the sensitization.

We have succeeded in preparing PbSe layers showing photoconductivity and internal photovoltaic effects at room temperature. The method of production is sufficiently reproducible, but there appears to be some room for improvement.

Method of production. The sensitive layers about 0·5 μ thick were formed in a hard glass envelope connected to the standard vacuum system. The electrical contact with the layer was provided by "aquadag" electrodes connected to tungsten leads sealed into glass walls.

Lead selenide containing up to 5% of an excess of lead over the stoichiometric proportion, prepared from pure elements by heating in vacuo, was used as the starting material. About 1 mg was used to form a layer by evaporation in vacuo or in oxygen at low pressure (about 0·01 mm Hg). The method of sensitization consisted in the exposure of the layer to oxygen at low pressure and heating it subsequently in vacuo at temperatures up to 450° C, followed by rapid cooling of the layer to room temperature. These treatments were controlled by measurements of the electrical conductivity, the photoconductivity and the thermoelectric power of the layer.

A layer showing photoconductivity when kept for a few minutes in vacuo at 300° C, connected to the external *emf* source (current of the order of 1 mA), acquires internal photovoltaic sensitivity when quickly cooled to room temperature. The direction of the photocurrent is opposite to that of the activating current.

After sensitization, the cells were cut off from the system and kept under vacuum, remaining stable for periods of many months.

Discussion of results. There is a general similarity between the behaviour of PbSe and PbS. The main difference is the much greater difficulty in removing the oxygen centres from the layer by heating it in vacuo. Layers evaporated in vacuo have negative thermoelectric power. The *n*-type conductivity of such layers is due to the presence of an excess of lead in the original material. Under the influence of oxygen at low pressure, even at room temperature, the conductivity changes to the *p*-type. Prolonged heating in vacuo at 400° C removes oxygen centres and changes the conductivity back to the *n*-type.

The photovoltaic activation at 300° C shows that oxygen centres are sufficiently mobile at this temperature to be moved by an applied field. The most sensitive layers were those of the lowest conductivity (about 0·01 mhos cm^{-1}) of dominant *p*-type, whereas *n*-type layers showed only a very poor sensitivity. There is, however, not any one-to-one relation between conductivity and photosensitivity.

This behaviour and the occurrence of the internal photovoltaic effect fits well into the barrier-theory picture. Independent confirmation is provided by Hall effect measurements made by M. Kozłowski (unpublished private communication) indicating very low mobility both of holes and electrons as compared with single crystals of PbSe.

Properties of photoconductive layers. The following characteristics were chosen as measure of quality of the cells:

1) The global reactivity defined as the ratio of the magnitude of the signal measured in μV, to the incident radiation energy in $\mu W/cm^2$.

2) Sensitivity being of the order of 10^{-8} W/cm^2, radiation from a black body source at 200° C was chopped at the rate of 800 c/s; signals from the cell were measured at the output terminals of a selective amplifier of 30 c/s band width. Results for several cells at room temperature are presented in the following table:

Number of the cells	Global reactivity in $\mu V/\mu W/cm^2$ current of the 500 μA.	Limiting sensitivity in W/cm^2
20	76·5	14×10^{-8}
32	47·5	22×10^{-8}
31	2·3	$7{\cdot}5 \times 10^{-8}$
33	128	$5{\cdot}5 \times 10^{-8}$

3) Spectral sensitivity for these layers was in the $0{\cdot}5\mu - 3{\cdot}6\mu$ wavelength range; it is shown in Fig. 1. Curve "*a*" corresponds to a standard cell, curve "*b*" to a cell made in the envelope provided with a very thin glass window (about 0·3 mm). The difference between these two curves indicates strong absorption by glass in the neighbourhood of 3μ.

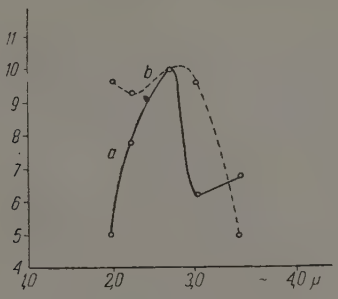

Fig. 1

Measurements under 1), 2), and 3) were made jointly by T. Piwkowski and the authoress.

Room temperature sensitivity to the total radiation from an ordinary incandescent electric lamp is more than 10 times less than that of an average PbS cell. On cooling the layer to about -130°C the sensitivity of some cells increases up to 10 times that at room temperature. No systematic investigations of the sensitivity dependence on temperature were performed.

Grateful acknowledgments are made to Prof. S. Pieńkowski for enabling the authoress to accomplish this work and to Prof. L. Sosnowski for his continued interest and many valuable suggestions given during its prosecution.

REFERENCES

[1] Sosnowski L., Starkiewicz J., Simpson O., *Photovoltaic Effects Exhibited in High Resistance Semiconducting Films*, Nature **158** (1946), 28.

[2] Sosnowski L., Starkiewicz J., Simpson O., *Lead Sulphide Photoconductive Cells*, Nature **159** (1947), 818.

[3] Sosnowski L., *Badania nad zjawiskami fotoelektrycznymi w półprzewodnikach*, T. N. W., 1949.

[4] Simpson O., Nature **160** (1947), 791.

[5] Blackwell D. E., Simpson O., Nature **160** (1947), 793.

[6] Starkiewicz J., Journal Opt. Soc. of America (1948), 481.

[7] Chasmar R., Nature **161** (1948), 281.

BULLETIN DE L'ACADÉMIE
POLONAISE DES SCIENCES
Cl. III — Vol. I, Nos 3—4, 1953

Experimental Evidence that ^{90}Y is not a Pure Beta-Emitter

by
B. MAKIEJ

Communicated by H. NIEWODNICZAŃSKI at the meeting of October 20, 1952

A radioactive nucleus which goes through beta-transition to the ground state is commonly called a "pure beta-emitter" although it emits the weak continuous gamma-radiation, first discovered by Aston (1927) in his measurements on RaE. Such gamma-radiation has been called "internal bremsstrahlung" (henceforth denoted by *IB*). An *IB* theory was postulated independently by Knipp and Uhlenbeck (1936) and by F. Bloch (1936), who showed quantum-mechanically that continuous radiation could be attributed to a sudden change in the nuclear charge which occurs when the beta-particle is created and leaves the nucleus. The *IB* theory was extended by Chang and Falkoff (1949) to the forbidden beta-transitions and for the different relativistically invariant interactions which might be used in the beta-decay theory. The *IB* spectrum was investigated and compared with this theory, among others, by Wu (1941) and more recently by Madansky and Rasetti (1951), Storruste (1951) and Makiej (1952). In the last-quoted work the author found close agreement between the *IB* theory and the experiment for ^{32}P, but there appeared to be no such agreement for gamma-radiation emitted by ^{90}Y. This conclusion was reached on the basis of a comparison of the experimental absorption curves of gamma-rays from ^{32}P and from ^{90}Y with those which were theoretically expected.

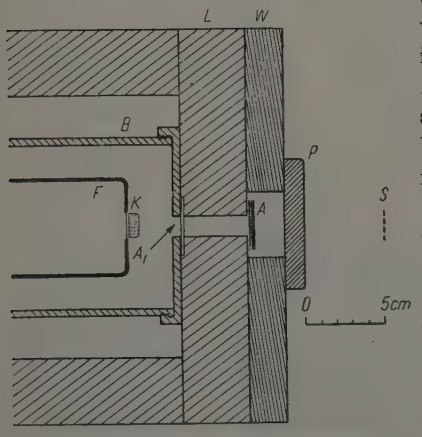

Fig. 1. Arrangement of apparatus

The experimental arrangement is shown schematically in Fig. 1.

The radioactive source is placed at *S*. The scintillation counter with photomultiplier *F* of the 11 stages *EMI* 5031 type and with natural sheelite phosphor *K* is used as detector for gamma-rays. The photomultiplier is covered by a light-proof brass box *B* with an aluminium foil window in front of the phosphor. In order to reduce the X-ray background, the surface of the lead shielding *L* facing the source is protected by a layer of wood *W*, which has an opening for the insertion of absorbers *A*. A block of paraffin-wax *P*, 1·2 cm thick, prevents the direct beam of beta-particles from reaching the counter. When the beta-absorber is in this position, one can easily see that the number of X-ray photons which are excited during absorption of the beta-particles and which reach the counter is negligible. In an experiment performed by C. S. Wu (1941), a ^{32}P-source was placed between two pieces of aluminium which served as beta absorbers. Because of this geometrical condition the intensity of *IB* was only one fourth the value of the X-rays excited in the beta-absorber. In our experiments the analogous ratio amounted to 10 for ^{32}P (3 mg/cm^2) and to about 2 for ^{90}Y (50 mg/cm^2), owing to a better geometrical arrangement and to a lower effective atomic number of the beta-absorber.

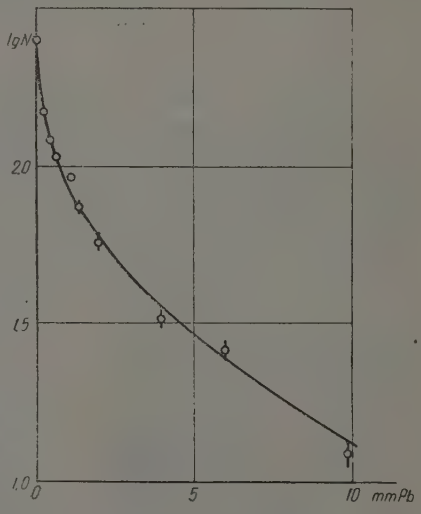

Fig. 2. Absorption in lead of the internal bremsstrahlung of ^{32}P

The results of the absorption measurements and calculations are given in Figs. 2 and 3.

The curve plotted in Fig. 2 represents the theoretically expected absorption in lead of the *IB* from ^{32}P ($T = 14{\cdot}3^d$, $E = 1{\cdot}71$ MeV) which, for the purpose of simplification, is calculated on the assumption that the efficiency of the counter remains constant within a detection interval ranging from 0·08 MeV to 1·5 MeV. The experimental results corrected for X-rays and absorption in the paraffin-wax block are marked by circles; allowing for experimental errors they follow closely the theoretical curve, thereby confirming the theory of Knipp and Uhlenbeck.

The theoretical absorption curve of the *IB* from ^{90}Y ($T = 60{\cdot}5^h$, $E = 2{\cdot}18$ MeV) and the experimental absorption curve of gamma-rays emitted by ^{90}Y were obtained in the same way as for ^{32}P.

A glance at Fig. 3 shows that the slope of theoretical curve *B* is much steeper than that of experimental curve *A*. This means that the gamma radiation emitted by ^{90}Y is harder than would be expected under the *IB* theory. Investigations by various workers would seem to bear out that the *IB* theory is at least approximately correct, so that the gamma-radiation emitted by ^{90}Y must consist of both *IB* and genuine gamma rays.

Several absorption curves were taken over a period lasting for more than 3 half-lives, but there was no noticeable difference in the shape of the curves. Therefore the half-life of the transitions in which genuine gamma-rays are created is equal to the half-life of the beta transitions ^{90}Y, ^{90}Zr. As interference by radioactive impurities with exactly the same half-life is very improbable, one is forced to conclude that some of the beta-transitions go

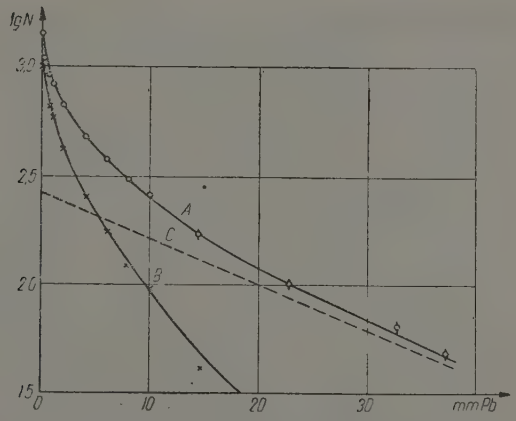

Fig. 3. Analysed absorption curve in lead of gamma-rays from ^{90}Y

to an excited state of ^{90}Zr and are immediately followed by a gamma-ray Consequently ^{90}Y is not a pure beta emitter as has been commonly regarded (Djelepof and Petrovich, 1950). The simplest assumption is to ascribe the hard component of the absorption curve (*A*) as due mainly to genuine monoenergetic gamma radiation. Indeed, as may be seen from Fig. 3, one can decompose the experimental results graphically into two different parts: the first being that whose logarithms lie on the straight line (*C*), and the second (oblique crosses in Fig. 3) being that which follows the theoretical absorption curve (*B*). According to this analysis a rough estimate of genuine gamma radiation of ^{90}Y gives about 5 photons of 1.5 MeV energy per 10 000 beta-transitions.

This report is based on experiments performed by the author in the Physics Department, University of Birmingham to the Directors of which,

Professors M. L. Oliphant and P. B. Moon, the author wishes to express his best thanks. The author is also indebted to Professor H. Niewodniczański for many helpful discussions.

Physical Laboratory, Jagiellonian University, Cracow

REFERENCES

[1] Aston G. H., Proc. Camb. Phil. Soc. **23** (1927), 953.
[2] Bloch F., Phys. Rev. **50** (1936), 272.
[3] Chang C. S. W. and Falkoff D. L., Phys. Rev. **76** (1949), 365.
[4] Djelepof B. and Petrovich S., UFN, **40** (1950), 497.
[5] Knipp J. K. and Uhlenbeck G. E., Physica **3** (1936), 425.
[6] Madansky L. and Rasetti F., Phys. Rev. **83** (1951), 187.
[7] Makiej B., Acta Physica Polonica, **11** (1952), in print.
[8] Storruste A., Meddelelse No 185 fra Universitetets Fysiske Institutt, Oslo (1951).
[9] Wu C. S., Phys. Rev. **59** (1941), 481.

BULLETIN DE L'ACADÉMIE
POLONAISE DES SCIENCES
Cl. III — Vol. I, Nos 3—4, 1953

CHEMISTRY

Magnetic Properties of Titanium Hydrides

by

W. TRZEBIATOWSKI and B. STALIŃSKI

Communicated by W. TRZEBIATOWSKI at the meeting of January 12, 1953

A systematic magnetochemical investigation of the titanium-hydrogen system through the entire composition range from Ti to $TiH_{1.98}$ was undertaken. The hydrides were prepared in a vacuum apparatus through the action of known volumes of hydrogen evolved from palladium or titanium hydrides on samples of pure, spongy titanium (99·5 %), practically free from ferromagnetic impurities. The composition of the hydrides was controlled by chemical analysis whose results are in agreement with those calculated from the gas volumes. A total of 24 samples, which covered the entire composition range, was prepared. Their crystal structure was controlled by powder diagrams, using CuK_α or TiK_α radiation, and lattice constant measurements of the α- and β-phases [1]-[3]. In addition 3 samples of titanium deuterides $TiD_{1.57}$, $TiD_{1.86}$ and $TiD_{1.94}$ were prepared in the same manner, using deuterium obtained by electrolysis from heavy water (99·65 % D_2O). The susceptibility of the samples was measured by the Gouy method using 2 g samples and magnetic field intensities of 4090, 6610, 8190 and 9550 Oe in the temperature range from 80° to 300°K and in some cases to 470°K. Only for 3 samples did the extrapolated values ($H \to \infty$) of the susceptibility coefficient result in a decrease of 2 to 3 %. The remainder gave differences only within the limits of experimental error ($\pm$ 0·5 %). As standard substance a solution of 20·01 % $NiCl_2$ was used ($\chi_{+20°} = 6{\cdot}32 \times 10^{-6}$). The results are presented in Figs. 1 and 2.

The results show that the paramagnetic susceptibility of titanium metal ($\chi_{g+18°} = +3{\cdot}18 \times 10^{-6}$) is increased as a result of hydrogen solution. This increase, previously stated only for one composition [4], is in the range of α and $\alpha + \beta$ phases, more or less proportional to the hydrogen concentration, but the temperature increment of susceptibility decreases slightly. The diffraction pattern of the α-phase disappears completely at $TiH_{1.07}$. The β-phase is already visible as $TiH_{0.46}$. The β-phase first shows a certain delay in the increase of the susceptibility isotherms and then, with a higher hydrogen content, a normal increase but a diminishing temperature coefficient.

At $TiH_{1\cdot8}$ a distinct maximum of susceptibility is observed and the temperature coefficient rises. At $TiH_{1\cdot9}$ a sharp minimum occurs, after which the hydrides reach their saturation limit at $TiH_{1\cdot98}$. At composition exceeding $TiH_{1\cdot70}$ a distinct maximum on the $\chi - T$ curves is visible at about 300°K. The solution of hydrogen in α — Ti does not markedly change the lattice

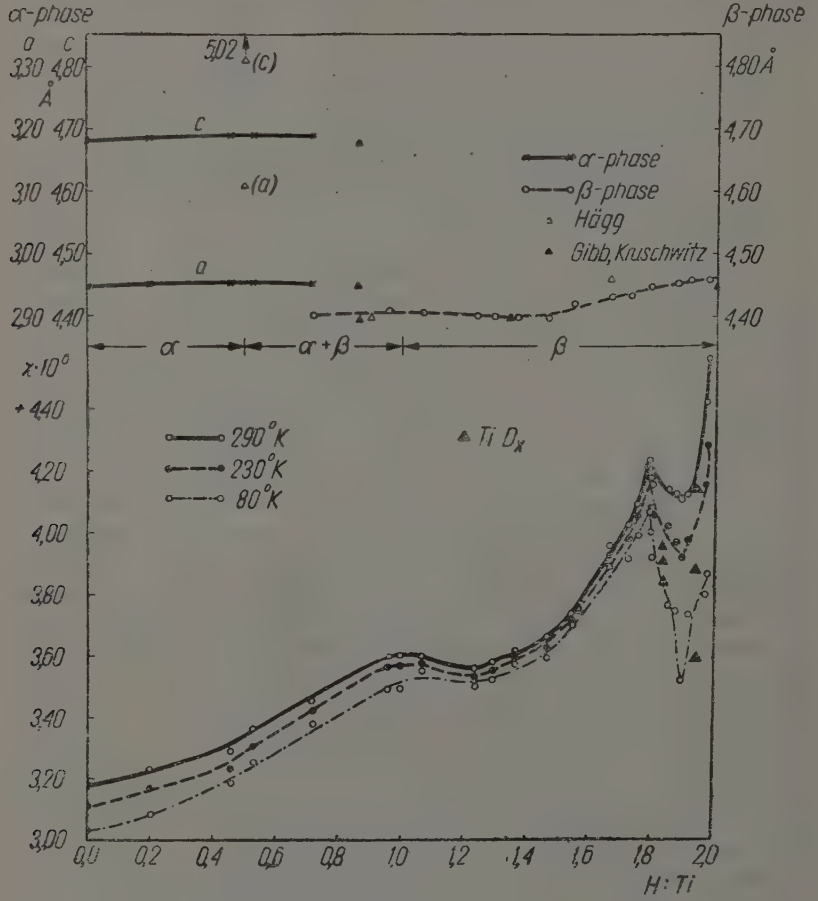

Fig. 1. Susceptibility isotherms and lattice constants of th Ti—H system

constant of the metal. An increase of these is evident for the β-phase at composition of more than $TiH_{1\cdot50}$. The properties of the titanium deuterides do not differ appreciably from those of corresponding hydrides.

From these measurements it is evident that the magnetic properties of titanium hydrides are much more complicated than those of the palladium hydrides, which have been extensively investigated [5—7]. Palladium shows,

with an increasing hydrogen content, a decrease in its paramagnetic susceptibility, which reaches zero at $PdH_{0.64}$ or $PdD_{0.66}$. This result was explained on the assumption that 0·6 holes/atom Pd of the *d*-band are filled with electrons released from dissolved hydrogen. In the *d*-band titanium probably also possesses about 3 electrons/atom that is less than palladium. One may expect that, with increasing hydrogen content, this number of electrons will rise, resulting

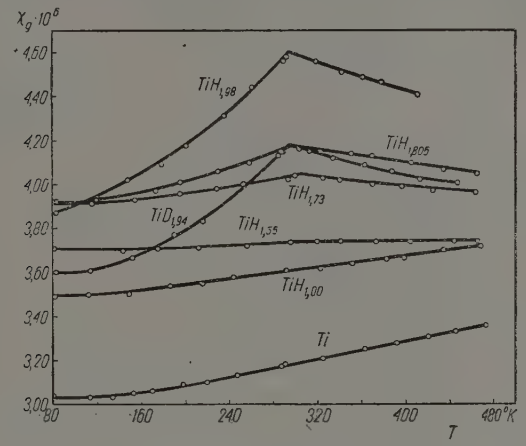

Fig. 2. Susceptilibity - temperature curves of some titanium hydrides and one titanium deuteride

at first in an increase, and, with a higher hydrogen content, in a decrease of the magnetic moment. But titanium, like other transition metals, does not follow the Curie-Weiss law, showing a positive temperature coefficient of susceptibility. For transition metals a strong interaction of *d*-electrons of adjacent atoms is accepted (antiferromagnetism) [8]. A direct proof of such interaction is the shape of the susceptibility temperature curve of the β-phase at hydrogen contents of more than $TiH_{1.7}$. The maxima of these curves occur at compositions at which the lattice constants rise, which always diminishes the electron coupling. The maximum and minimum observed on the susceptibility isotherms is probably the result of two factors: (1) the increase of the total number of electrons and (2) the decoupling of *d*-shells, both progressing with the hydrogen content.

Susceptibilities of titanium, titanium hydrides and deuterides

Composition															
°K	80	113	153	170	198	220	247	288	325	363	393	421	446	473	289
$Ti\ \chi \cdot 10^8$	304	303	305	306	309	310	313	317	321	325	328	331	333	339	317
	80	110	135	157	180	202	223	255	287						
$TiH_{0.20}$	308	307	308	311	311	313	316	319	322						
	80	116	145	175	218	257	291								
$TiH_{0.46}$	319	318	318	319	322	325	329								

Susceptibilities of titanium, titanium hydrides and deuterides (continued from p. 139)

Composition	°K														
$TiH_{0.53}$	80	113	138	175	215	234	265	292							
	326	325	325	327	330	331	333	336							
$TiH_{0.78}$	82	113	131	156	185	192	208	222	244	287					
	338	337	337	338	339	340	341	342	342	345					
$TiH_{0.96}$	80	110	140	176	206	221	244	291							
	349	351	352	353	355	356	358	360							
$TiH_{1.00}$	81	112	149	186	216	254	292	323	352	383	400	435	469	290	
	349	350	350	354	355	358	361	362	364	366	367	370	372	360	
$TiH_{1.07}$	80	110	150	170	205	238	263	291							
	356	354	355	355	356	358	359	360							
$TiH_{1.24}$	80	120	157	195	235	267	294								
	352	350	350	352	354	355	356								
$TiH_{1.295}$	80	119	148	194	228	260	295								
	354	352	352	354	355	356	358								
$TiH_{1.37}$	80	118	160	185	222	255	295								
	359	357	357	357	358	360	362								
$TiH_{1.47}$	80	116	148	185	223	255	289								
	360	359	359	360	363	364	366								
$TiH_{1.55}$	80	143	175	212	256	296	320	341	373	405	445	466	301		
	371	370	371	371	372	374	374	374	374	374	374	374	374		
$TiH_{1.67}$	81	117	154	184	225	258	292								
	390	389	390	391	394	394	395								
$TiH_{1.73}$	80	115	154	195	229	253	294	300	325	342	370	398	425		
	392	391	393	396	398	400	402	404	403	402	400	398	396		
$TiH_{1.76}$	81	118	157	200	262	300									
	399	400	401	404	409	410									
$TiH_{1.795}$	82	122	155	181	206	234	267	290	315	343	373	396	335	420	456	302
	406	409	411	413	415	417	421	424	423	422	420	418	422	418	417	424
$TiH_{1.80}$	80	119	159	189	221	250	291								
	401	401	401	403	407	411	417								
$TiH_{1.805}$	83	120	174	196	230	258	288	314	324	352	370	405	435	466	304	
	392	393	397	401	406	410	416	—	415	414	413	410	407	405	416	
$TiH_{1.855}$	80	113	143	173	206	243	296								
	377	379	386	390	397	406	416								
$TiH_{1.88}$	80	125	150	175	214	240	266	291							
	375	376	379	385	393	399	406	414							
$TiH_{1.90}$	82	115	145	174	215	252	295								
	351	360	367	374	387	400	411								
$TiH_{1.92}$	81	122	153	181	222	258	290								
	374	376	381	387	397	403	412								
$TiH_{1.975}$	82	118	150	180	201	245	290								
	380	383	390	399	403	422	442								
$TiH_{1.98}$	82	120	148	179	201	235	261	293	319	343	362	379	412	431	297	
	387	394	402	409	418	431	444	458	456	451	449	447	441	434	453	

Susceptibilities of titanium, titanium hydrides and deuterides (continued from p. 135)

Composition														
$TiD_{1.57}$	°K	81	113	135	171	204	251	288						
	$\chi \cdot 10^8$	375	373	373	373	374	373	376						
$TiD_{1.86}$	°K	83	114	157	190	221	250	291						
	$\chi \cdot 10^8$	384	382	382	384	387	390	395						
$TiD_{1.94}$	°K	82	114	152	190	216	253	285	304	314	335	364	388	415	448
	$\chi \cdot 10^8$	360	361	367	377	383	399	413	416	415	412	408	406	402	401

Institute of Technology, Department of Chemistry, Wroclaw

REFERENCES

[1] Hägg G., Ztsch. phys. Chem. B **11** (1931), 433.
[2] Gibb T. R. P., Kruschwitz H., J. Am. Chem. Soc. **72** (1950), 5365.
[3] Gibb T. R. P., Mc Sharry J. J., Bradgon R. W. J. Am. Chem. Soc. **73** (1951), 1751.
[4] Fitzwilliam J., Kaufmann A., Squire C., J. Chem. Phys. **9** (1941), 678.
[5] Svensson B., Ann. Phys. **18** (1933), 299.
[6] Sieverts A., Danz W., Ztsch. Phys. Chem. **B 38** (1937), 61.
[7] Wucher J., C. R. **229** (1949), 175.
[8] Zener C., Phys. Rev. **81** (1951), 440.

BULLETIN DE L'ACADÉMIE
POLONAISE DES SCIENCES
CL. III — Vol. I, Nos 3—4, 1953

CHEMISTRY

Properties of the Antimony Microelectrode in Aqueous Alcoholic Solutions

by

B. KAMIEŃSKI, Z. BYŁO and B. WALIGÓRA

Communicated by B. KAMIEŃSKI at the meeting of November 17, 1952

A. A. Szczerbakow [1], W. M. Clark [2], H. T. S. Britton [3], Getman and Daniels [4], G. A. Perley [5], Kolthoff and Furman [6], Parks and Beard [7] and others have contributed much to our understanding of the mechanism of the antimony electrode.

B. Kamieński applied the electrode to the study of potentiometric chromatography in 1949 (see references [8], [9] and [10]), using a special form of microelectrode. In the course of potentiometric chromatographic investigations different mixtures of alcohols with water were used, and it was necessary to study the behaviour of the antimony electrode when applying the device of B. Kamieński. The potential of the antimony electrode was measured after immersing it in a series of aqueous mixtures of methyl alcohol at different hydrogen ion concentrations, aftewards in aqueous mixtures of ethyl alcohol and finally in aqueous mixtures of propyl alcohol at different hydrogen ion concentrations. A one tenth normal potassium chloride calomel electrode was used as reference electrode and a quadrant electrometer of small electrical capacity served as measuring apparatus. The concentration of phosphate buffers ranged from 0·0044 to 0·022 moles per litre. Fig. 1 represents the influence of the hydrogen ion concentration on the potential of the electrode immersed in different mixtures of methyl alcohol with water. As may be seen from the figures, the greater the concentration of methyl alcohol the more negative is the potential, and a similar phenomenon is observed when ethanol is mixed with water (Fig. 2). The lines are almost straight, although an increasing curvature may be observed when the concentration of alcohol it greater (upper lines). The influence of the concentration of propanol is similar, as may be seen from Fig. 3.

The results of the measurements show that the application of the antimony microelectrode is possible in different alcoholic mixtures with water, and that small changes in the proportion of the binary mixture which may

occur during the adsorption analysis will not impair the accuracy of the results.

After testing the microelectrode described in former papers [8], [9], [10], the influence of weak acids and bases on the potential of the electrode was

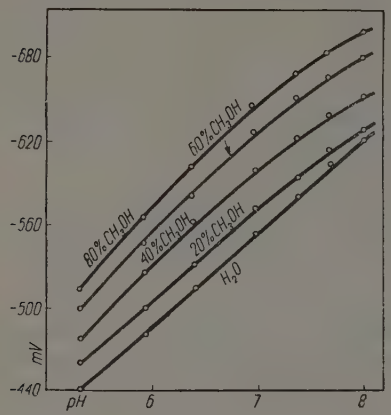

Fig. 1

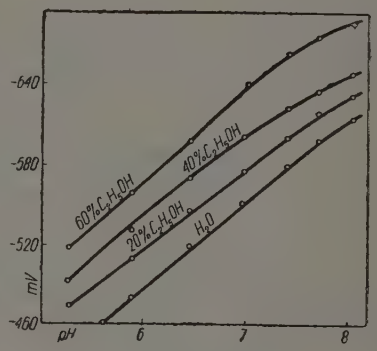

Fig. 2

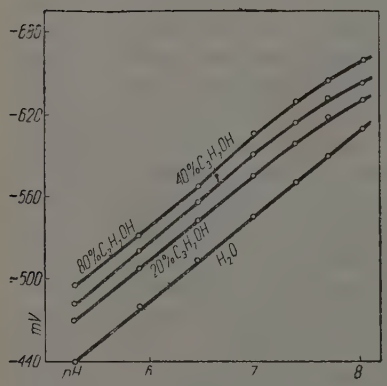

Fig. 3

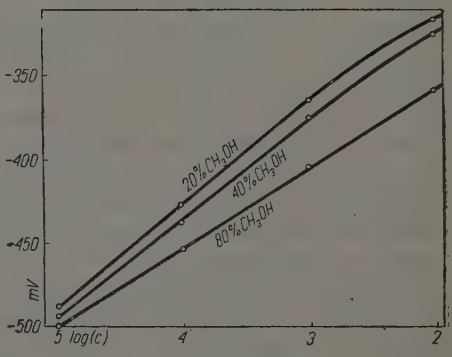

Fig. 4

investigated. The same solvent mixtures were used for this purpose. Fig. 4 represents the change of potential (ordinate) with the logarithm of concentration (abscissa) of propionic acid in aqueous solutions of 20%, 40% and 80% methanol. Similar measurements were carried out with butyric acid (Fig. 5), *n*-valerianic acid (Fig. 6), *n*-capronic acid (Fig. 7), *n*-oenanthic acid (Fig. 8), *n*-caprylic acid (Fig. 9) and *n*-myristic acid (Fig. 10).

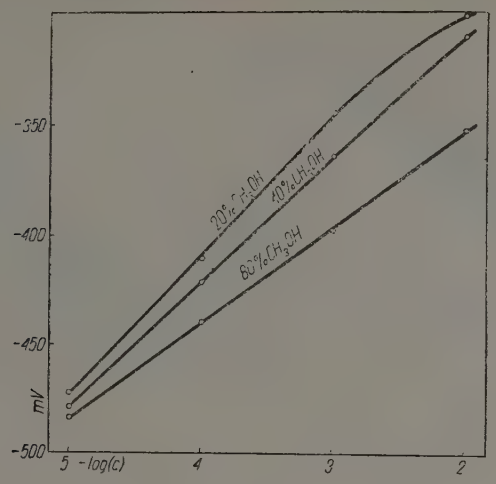

Fig. 5

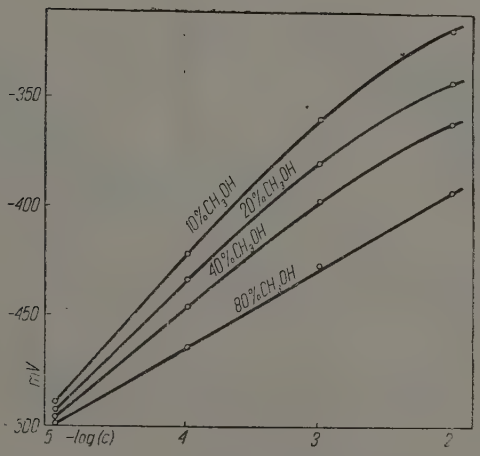

Fig. 6

A similar series of measurements was made with cinchonine (Fig. 11) and brucine (Fig. 12).

We may regard the measuremets hitherto described as a method of testing the microelectrode, and we emphasise that the electrode is a very sensitive device enabling us to detect very small quantities of acids and bases dissolved in mixtures of water with methanol or possibly ethanol or propanol with water in any proportion. It is interesting that, in spite of a fairly large change in the dielectric constant, hydrogen ions are readily detected by the antimony electrode, so that the device may be applied to a large number of various mixtures of solvents.

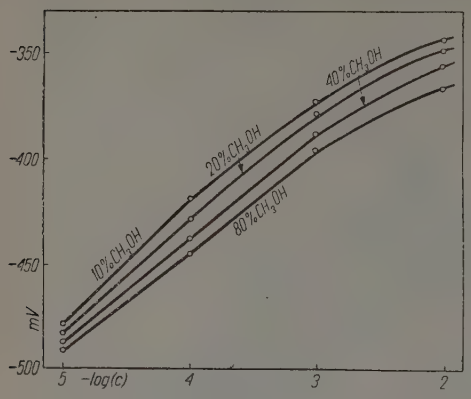

Fig. 7

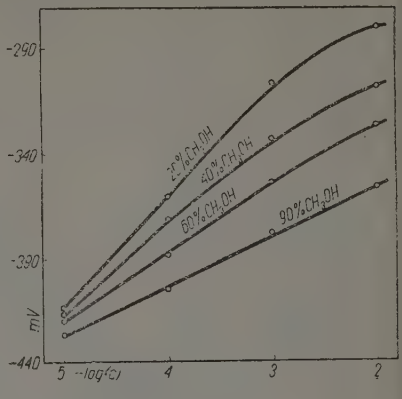

Fig. 8

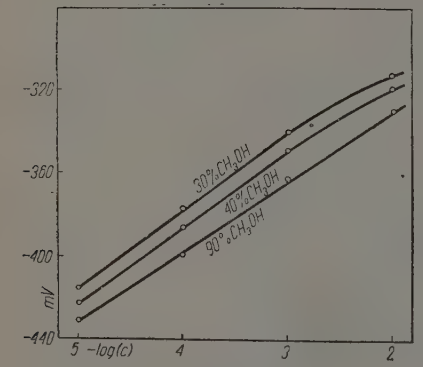

Fig. 9

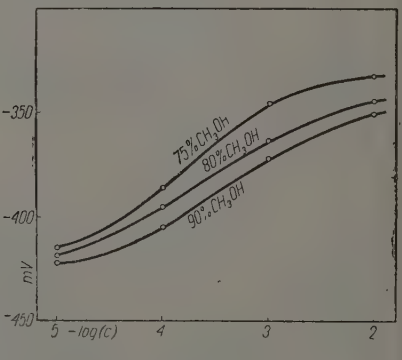

Fig. 10

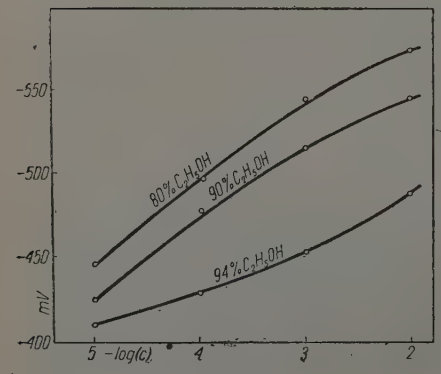

Fig. 11

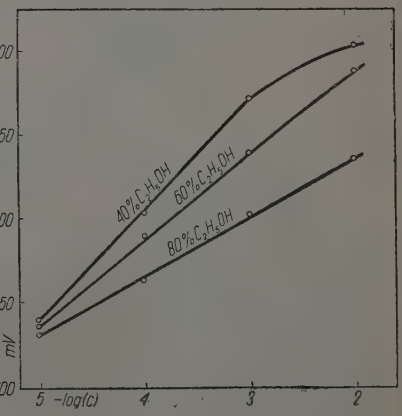

Fig. 12

REFERENCES

[1] Szczerbakow A. A., Żurnal Analiticzeskoi Chimii **6** (1951), 157.

[2] Clark W. M., *The determination of hydroden ions*, 3rd ed., Baltimore (1928), 424.

[3] Britton H. T. S., *Hygrogen ions*, 2nd ed. London 1932.

[4] Getman and Daniels, *Outlines of theoretical Chemistry*, 5th ed. New York, 1931, 474.

[5] Perley G. A., Ind. and Engl. Chem. Anal. Ed. **31** (1939), 319.

[6] Kolthoff and Furman, *Potentiometric Titrations*, 2nd ed. (1931).

[7] Parks and Beard, J. Am. Chem. Soc. **54** (1932), 856.

[8] Kamieński B., Bull. Int. Ac. Polon. A (1949), 131.

[9] Kamieński B., Bull. Int. Ac. Polon. A (1949), 173.

[10] Kamieński B., Acad. Polon., Rozprawy Wydziału Matem. Przyrodn. **74** Part A (1949), Seria III, **34** (1949), 1—41.

BULLETIN DE L'ACADÉMIE
POLONAISE DES SCIENCES
Cl. III — Vol. I, Nos 3—4, 1953

CHEMISTRY

Electrometric Adsorption Analysis of Strychnine and Brucine Potentiometric Chromatography

by
B. WALIGÓRA and Z. BYŁO

Communicated by B. KAMIEŃSKI at the meeting of November 17, 1952

In a former paper, "Potentiometric Chromatography. Part XVI", it was shown that aqueous solutions of alcohols may be used in the electrometric detection of weak acids and bases, if the antimony microelectrode of B. Kamieński (see references [1], [2], [3], [4], [5], [6], [7] and [8]) is applied as a measuring device. Here, in these measurements, the device was placed at the bottom of an adsorption tube filled with aluminium oxide (according to Brockmann). However, commercial aluminium oxide is alkaline and it is a rather troublesome process to purify the adsorbent. Fig. 1 represents the change of the alcaline reaction, when a small glass tube of 7 mm dia-

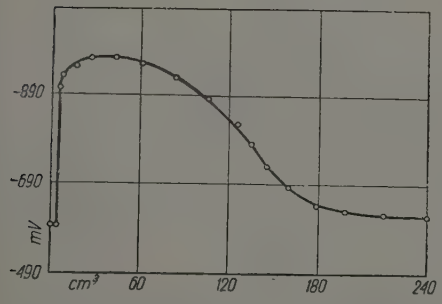

Fig. 1

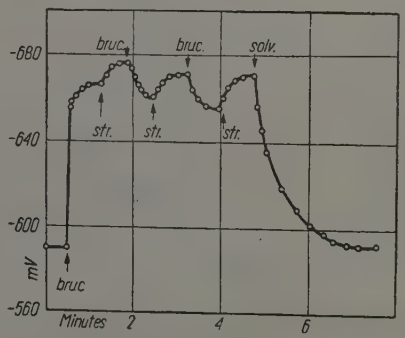

Fig. 2

meter was filled to a height of 15 mm with aluminium oxide and the column washed with 240 ccm (abscissa) of twice-distilled water. The microelectrode was inserted into the drops trickling out of the adsorption tube and the potential (ordinate) of the antimony electrode measured. To purify 250 g aluminium oxide, 40 days were needed and 75 litres of redistilled

water used. The purified aluminium oxide was dried at a temperature of 240° C for $5^1/_2$ hours.

Before applying this purified aluminium oxide, the reaction of the microelectrode to solutions of 0·397 mg brucine in 1 ccm of 70% ethanol and 0·334 mg strychnine in 1 ccm of the same solvent was tested. Fig. 2 represents the results of immersing the electrode alternately into the brucine

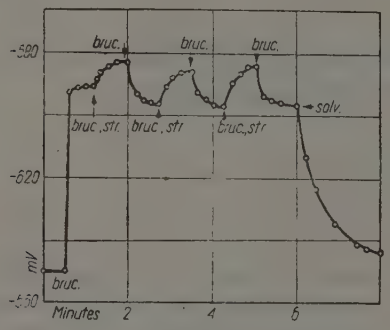

Fig. 3

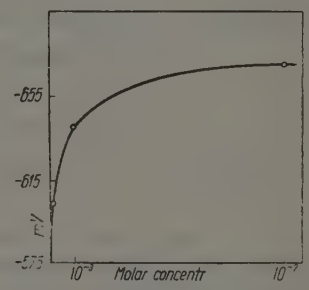

Fig. 4

and then into the strychnine solutions. The ordinate represents the potential, the abscissa the time. The arrows denote the moments of immersion and the washing of the electrode. Further characteristic behaviour of the system is shown in Fig. 3, when the electrode was put into a mixture of

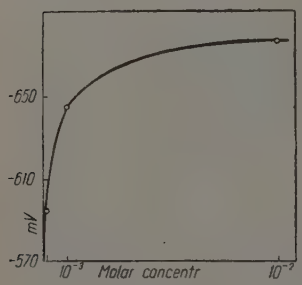

Fig. 5

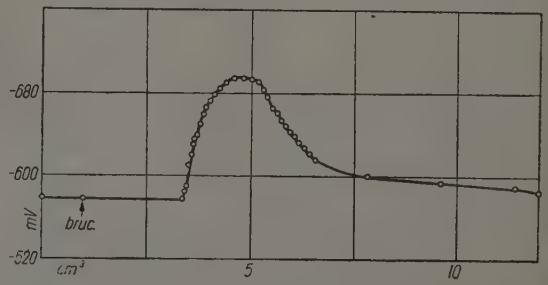

Fig. 6

strychnine and brucine (0·167 mg strychnine and 0·197 mg brucine in 1 ccm of solvent). The electrode was at first immersed in the brucine solution (concentration 0·397 mg in 1 ccm of 70% ethanol (see Fig. 3)), then in the mixture of strychnine and brucine, again in the brucine solution, and so forth, until finally the electrode was put into the solvent (70% ethanol). The moments of changing the solution are shown by arrows (Fig. 3). As may be seen, the action of brucine is feebler than that of strychnine and,

when brucine is mixed with strychnine, stronger action prevails. This behaviour indicates that a frontal adsorption analysis of strychnine and brucine mixtures should be possible. However, there is another important factor, namely that of alcaloid concentration. The influence of the concentration of brucine (Fig. 4) and of strychnine (Fig. 5) on the potential of the electrode was therefore examined. The action of strychnine is also somewhat stronger here, as may be seen in Fig. 4 and 5.

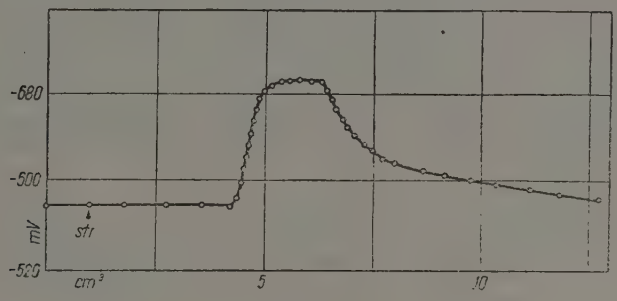

Fig. 7

The next step was to investigate the adsorption of brucine on a column of purified aluminium oxide. 1·97 mg brucine were dissolved in 1 ccm aqueous ethanol (50%) and added to the top of an aluminium oxide column, 100 mm

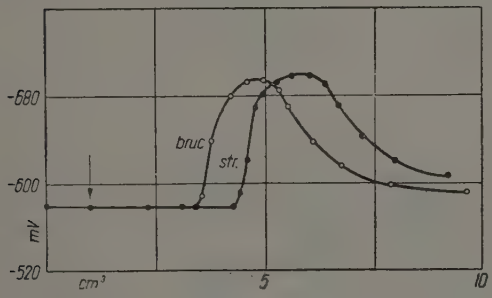

Fig. 8

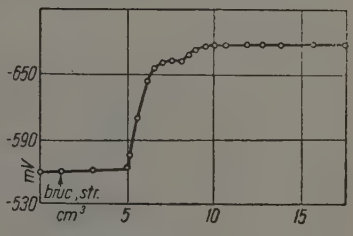

Fig. 9

high and 7 mm in diameter. When the last drops of the solution had entered the column, the eluent (50% ethanol) was poured into the column. Fig. 6 represents the results of the measurement which lasted 23 minutes. A similar experiment was made with 1·67 mg strychnine in 1 ccm of the mixed solvent and the results are shown in Fig. 7. It is evident that strychnine is more strongly adsorbed than brucine.

In order to compare the results of the measurements represented in Figs. 6 and 7, both diagrams are plotted together in Fig 8.

Using a similar column and a solution of 6·68 mg strychnine and 7·98 mg brucine in 25 ccm of 50% ethanol we carried out a frontal analysis; the results are shown in Fig 9. The experiment lasted 31 minutes. Much smaller quantities of the substances and solution are required when an elution analysis is made. Fig. 10 represents the following case: 1·67 mg

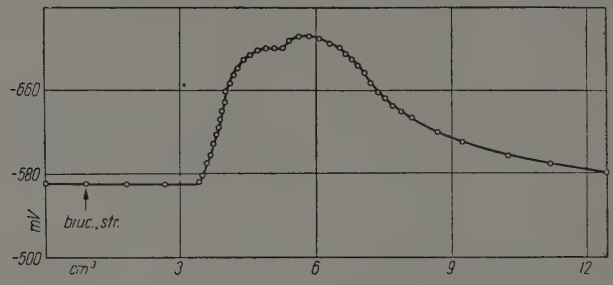

Fig. 10

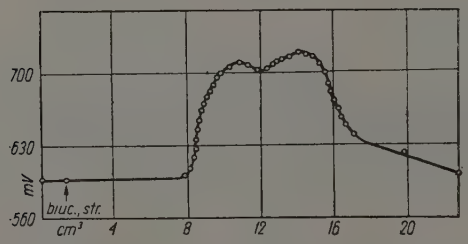

Fig. 11

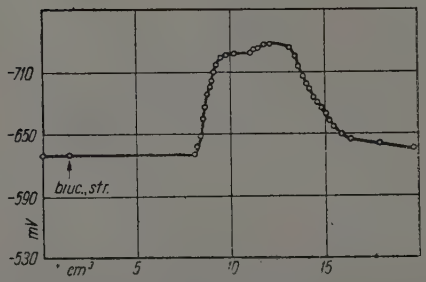

Fig. 12

strychnine and 1·87 mg brucine were dissolved in 2 ccm of 50% ethanol Putting this solution on the top of a similar column and eluting it with 50% ethanol the first traces of separation were observed after 25½ minutes, as may be seen from Fig. 10.

When the height of the column was doubled (to 200 mm), the separation was more marked, as may be seen from Fig. 11. The experiment lasted much longer, namely 61 minutes. A further tenfold decrease of concentration (0·167 mg strychnine + 0·187 mg brucine in 2 ccm methanol) and a change of the solvent into 20% methanol gave the result represented in Fig. 12. From an examination of the figure it becomes evident that, in spite of the strong dilution, the change of the potential is well marked, notwithstanding the fact that a column of the same height was used. The experiment lasted somewhat longer, namely 69 minutes.

The earlier observations of B. Kamieński on the slight influence of the dilution of solutions on the potential were confirmed and it may be emphasized that the sensibility of the electrometric method is very great even when very dilute solutions are used.

REFERENCES

[1] Kamieński B., Bull. Int. Acad. Polon. A Nr 7—10 (1948), 127—133.

[2] Kamieński B., Bull. Int. Acad. Polon. A Nr 1—4 (1949), 75—80. ibid. (1949), 81—86; ibid. (1949), 87—89.

[3] Kamieński B., Bull. Int. Acad. Polon. A (1949), 157—160; ibid. (1949), 171—182.

[4] Kamieński B., Bull. Int. Acad. Polon. A Nr 1—10 (1950), 73—77.

[5] Kamieński B., Acad. Polon., Rozprawy Wydziału Matemat.-Przyrod. **74** Part. A (1949), Seria III, **34** Nr 3 (1949), 1—41.

[6] Kamieński B., Było Z., Waligóra B., Bull. Int. Acad. Polon. A (1951), 199—222.

[7] Kamieński B., Waligóra B., Bull. Int. Acad. Polon. A (1951), 223—229.

[8] Kamieński B., Było Z., Bull. Int. Acad. Polon. A (1951) 231—237.

BULLETIN DE L'ACADÉMIE
POLONAISE DES SCIENCES
Cl. III — Vol. I, Nos 3—4, 1953

CHEMISTRY

Binary Eutectics Formed by One Component with a Series of Homologues

by

T. PENKALA

Communicated by W. ŚWIĘTOSŁAWSKI at the meeting of January 12, 1953

Several years ago W. Świętosławski [1] published a paper in which a series of binary eutectics, formed by a certain compound with a series of chemically quite different substances, were presented in one diagram. It was found that the eutectic points lay practically on a monotonic, continuous curve. Basing himself on this observation, Świętosławski came to the conclusions that if eutectics formed by component *A* with a series (*B*) of

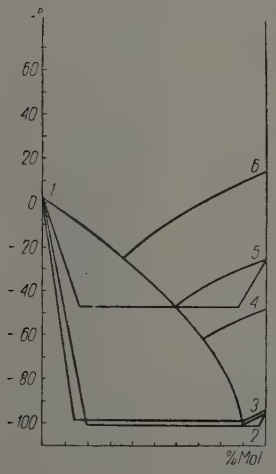

Fig. 1

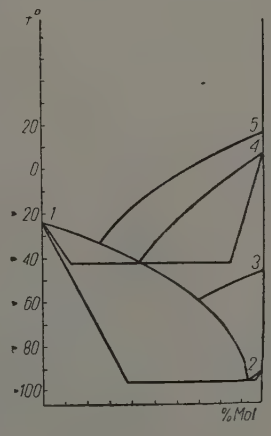

Fig. 2

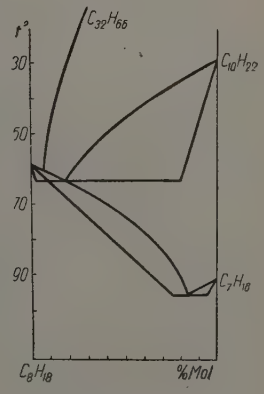

Fig. 3

Fig. 1. Eutectics formed by benzene (1) with toluene (2), ethyltoluene (3), metaxylene (4), orthoxylene (5) and paraxylene (6), according to Kravchenko's observations

Fig. 2. Eutectics formed by orthoxylene (1) with toluene (2), metaxylene (3), benzene (4) and paraxylene (5)

Fig. 3. Eutectics formed by paraxylene (1) with toluene (2), ethylbenzene (3), metaxylene (4), orthoxylene (5) and benzene (6)

homologues were examined, the curve on which the eutectic points would lie, would form a common curve corresponding to the well known freezing curve.

This note gives a series of examples which not only confirm Świętosławski's suggestion, but also lead to its further extension to those systems in which the eutectics are formed by two solid solutions, and not by two pure components, coexisting with the liquid phase in ideal eutectic systems.

In Figs. 1, 2 and 3 illustrations are given proving the correctness of Świętosławski's statements and of their further extension.

The examples given above refer to systems formed exclusively by different combinations of homologues of benzene and by benzene itself. A number of other examples have been found and will be described in a paper to be published in "Roczniki Chemii".

In the case of systems formed by paraffinic hydrocarbons: (C_8H_{18}, C_7H_{16}), (C_8H_{18}, $C_{10}H_{22}$), ($C_{10}H_{22}$, C_8H_{18}), ($C_{10}H_{22}$, C_7H_{16}) the eutectic points lie on the common freezing point of component *A* (3).

Department of Physical Chemistry, University of Warsaw

REFERENCES

[1] Świętosławski W., Roczniki Chem. **23** (1949), 1.

[2] Świętosławski W., *Metody rozdzielania i oczyszczania substancji*, Warszawa, 1950.

[3] Kravchenko B. M., Żurn. Prikł. Chim. **22** (1949), 491, 724.

BULLETIN DE L'ACADÉMIE
POLONAISE DES SCIENCES
Cl. III — Vol. I, Nos 3—4, 1953

CHEMISTRY

Binary Solid Solutions and Eutectic Mixtures Formed by One Component with Representatives of a Series of Homologues

by

T. PENKALA

Communicated by W. ŚWIĘTOSŁAWSKI *at the meeting of January 12, 1953*

Some time ago W. Świętosławski [1] published a paper in which he suggested that the examination of binary mixtures formed by substance A with representatives of a series of homologues, B, B_1, $B_2 \ldots B_n$, showed a gradual transition from ideal eutectics (pure components in solid phases), through eutectics of solid solutions, to solid solutions characterised by unlimited mutual solubility (Fig. 1).

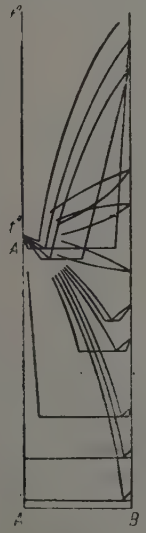

Fig. 1

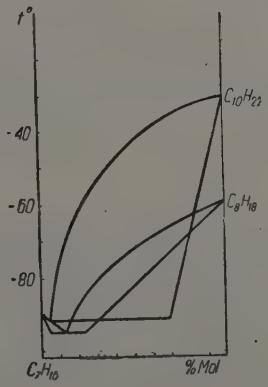

Fig. 2

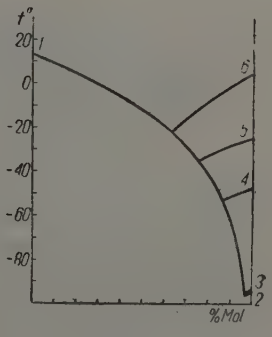

Fig. 3

Fig. 1. Gradual transition from eutectics to solid solutions according to the scheme given by Świętosławski. The upper part of the diagram is extended to cases in which the higher melting representatives of the series form eutectics with component A

Fig. 2. Eutectics formed by *n*-heptane

Fig. 3. Eutectics formed by *n*-decane

Świętosławski's suggestion is now confirmed and extended. A gradual transition really occurs in the series of paraffins and depends on the differences in length of the carbon atom chains.

The extension of the diagram given in 1949 by Świętosławski consists in the addition of the upper part, in which component A, characterised by relatively low melting point t_A, forms eutectics with the representatives with considerably higher melting points.

In Figs. 2 and 3 all the combinations formed by n-heptane, n-octane and n-decane are shown. In addition the diagram shown in Fig. 4 demon-

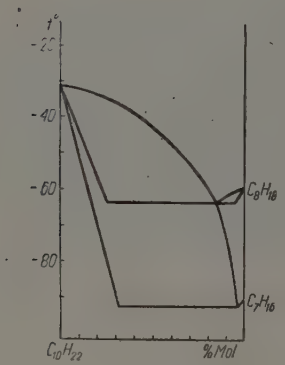

Fig 4. Eutectics formed by n-octane with three other paraffins. $C_{32}H_{66}$ forms an ideal eutectic, the two other non-ideal ones

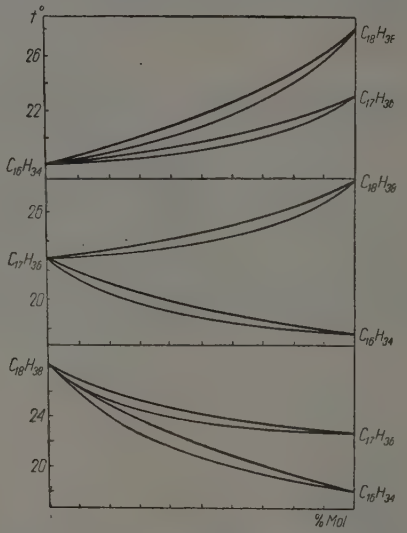

Fig. 5. A series of solid solutions formed by paraffins

strates that the eutectic points lie on one curve independently of whether the solid phases are pure components or solid solutions.

Seyer [3] showed that the systems formed by (C_4H_{10}, $C_{32}H_{66}$) (C_6H_{14}, $C_{32}H_{66}$), (C_8H_{18}, $C_{32}H_{66}$), ($C_{16}H_{34}$, $C_{32}H_{66}$) and ($C_{20}H_{42}$, $C_{32}H_{66}$) are eutectics due to the large differences in the length of the chains.

The same phenomena take place in other binary mixtures if, for instance, substance A does not belong to the same series of homologues.

Chlorobenzene, bromobenzene and iodobenzene form with each other solid solutions characterised by their unlimited solubility; with fluorobenzene, however, systems with limited solubility appear. This is associated with a considerable difference in the size of the atoms involved.

Similar phenomena are observed in many other cases and discussed in a paper to be published shortly in "Roczniki Chemii". In all these cases a gradual transition takes place from solid solutions with unlimited solubility torugh those characterised by a limited solubility to ideal eutectics.

Department of Physical Chemistry, University of Warsaw

REFERENCES

[1] Świętosławski W., Roczniki Chemii **23** (1949), 7. *Metody rozdzielania oczyszczania substancji,* Warszawa, 1950.
[2] Kravchenko B. M., Żurn. Prikł. Chim. **22** (1949), 491.
[3] Seyer W. F., J. Am. Soc. **60** (1938), 827.

BULLETIN DE L'ACADÉMIE
POLONAISE DES SCIENCES
CI. III — Vol. I, Nos 3—4, 1953

CHEMISTRY

Adsorption of Dibenzyl Sulphoxide on Metals

by

M. ŚMIAŁOWSKI and Z. SZKLARSKA-ŚMIAŁOWSKA

Communicated by M. ŚMIAŁOWSKI at the meeting of January 19, 1953

Dibenzyl sulphoxide is known as a very effective corrosion inhibitor for metals in both sulphuric and hydrochloric acids. Since the protection of metals against the corroding action of acids, is generally supposed when organic inhibitors are used, to be due to adsorption of the inhibitor on the surface of the metal, many efforts have been made to determine the amount of adsorption of various organic compounds on metals. Thus Koshurnikov [1] measured the amount of adsorption of phenol on iron, Greenhill [2] and Hackerman and Cook [3] studied the adsorption and desorption isotherms of several long chain polar compounds on steel powder, and Śmiałowski, Synowiec and Szota [4] determined the amount of adsorption of aniline and diphenylamine on electrolytic iron powder. So far no measurements have been made in connection with typical corrosion inhibitors, such as dibenzyl sulphoxide, owing to the difficulty of determining accurately very small changes in weight or in solution concentration. Nothing is yet known concerning the heat evolved by the adsorption of organic compounds on metals.

In our present study we used the spectrophotometric method for determining the concentration of dibenzyl sulphoxide in solution. We found that concentrations of 0·001 to 0·015 g dibenzyl sulphoxide in 1000 g aqueous solution gave maximum extinction of ultraviolet radiation at 2140 to 2160 *A* wave-length. In this way it was possible to determine changes in concentration due to the adsorption of dibenzyl sulphoxide from water solutions on copper and nickel powders. No satisfactory results were obtained with iron powder.

We used electrolytically obtained metal powders, freshly heated in hydrogen atmosphere at 500° C. The average diameter of the grains of copper powder used in our experiments was less than 0·06 mm, and that of nickel powder less than 0·15 mm.

In each experiment 5 g of copper powder or 12 g of nickel powder were mixed with 10 ml of aqueous solution with a known concentration of dibenzyl sulphoxide. The mixture was shaken for 10 minutes at a constant

temperature. That period was sufficient to establish the equilibrium. Then 4 ml of solution, separated from the metal powder by centrifugation, were placed in the quartz vessel of the spectrophotometer (Unicam Cambridge) and the transmission of ultraviolet light was measured with reference to pure water. Comparison with the transmission value obtained for freshly prepared initial solution made it possible to determine the change of concentration with the desired accuracy.

In order to study the process of desorption, the metal powder after having been separated from a solution of a given concentration, was washed with a certain amount of water. After filtration the amount of dibenzyl sulphoxide present in the filtrate thus obtained was determined.

Figs. 1 and 2 show the adsorption isotherms of dibenzyl sulphoxide on copper and nickel powder from water solutions. The degree of accuracy

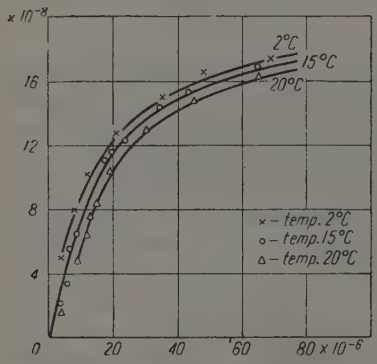

Fig. 1. 2° C, 15° C and 40° C isotherms of adsorption of dibenzyl sulphoxide on copper powder

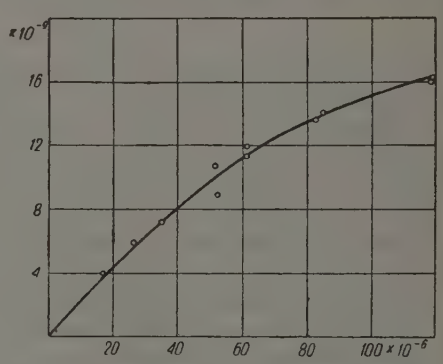

Fig. 2. 15° C isotherm of adsorption of dibenzyl sulphoxide on nickel powder

obtained in the measurements for copper was sufficient to enable us to determine the influence of temperature on the amount of adsorption. In the case of nickel no distinct effect was observed as a result of the rise in temperature from 2° C to 40° C. This was probably due to the fact that the area of nickel powder was smaller and hence there were greater errors in the measurements.

The study of the desorption of dibenzyl sulphoxide from the surface of copper and nickel powders showed that adsorption was reversible.

The data obtained for copper enabled us to calculate by means of the Clausius and Clapeyron equation, the approximative value of the adsorption heat of dibenzyl sulphoxide from water solutions;

$$\log \frac{a_2}{a_1} = \frac{\Delta H_a (T_2 - T_1)}{2{\cdot}303\, R\, T_1\, T_2}$$

a_1 — adsorption value at T_1
a_2 — adsorption value at T_2
R — gas constant
ΔH_a — enthalpy of adsorption.

The calculated values of ΔH_a are within the limits of 0·5 kcal per mole for stronger solutions and 1·7 kcal per mole for weak solutions of dibenzyl sulphoxide. This low value for the heat of adsorption seems to indicate that the phenomenon in question is rather an example of physical adsorption than of chemisorption.

REFERENCES

[1] Koshurnikov G. S., Żurn. Obszczej Chimii **18** (1948), 388.
[2] Greenhill E. B., Trans. Faraday Soc. **45** (1949), 625.
[3] Hackerman N. and Cook E. L., J. Electrochem. Soc., **97** (1950), 1.
[4] Śmiałowski M., Synowiec J., Szota M., Prace Główn. Inst. Metalurgii **2** (1950), 31.

BULLETIN DE L'ACADÉMIE
POLONAISE DES SCIENCES
Cl. III — Vol. I, Nos 3—4, 1953

CHEMISTRY

Evaluation of Diffusion of Hydrogen into Iron by Observation of Linear Expansion of a Sample

by

M. ŚMIAŁOWSKI and Z. SZKLARSKA-ŚMIAŁOWSKA

Communicated by M. ŚMIAŁOWSKI at the meeting of January 19, 1953

Although the phenomena of the penetration of nascent hydrogen into iron and steel during pickling in acids, or electrolysis of water solutions with an iron cathode, are well known, we have comparatively little information concerning the kinetics and mechanism of these processes.

For the purpose of studying the rate of diffusion of hydrogen through iron and steel, the majority of authors have used a method involving the evolution of gas on one side of a fine wall of the given material and the observation of the rise in pressure on the other side of the wall. Rather unsatisfactory results have been obtained in this way. Bodenstein [1], Borelius [2], Baukloh and Zimmermann [3], and Baukloh and Retzlaff [4] reported fluctuations in the observed rate of diffusion within large limits but gave no satisfactory explanation of this behaviour of iron and hydrogen. They emphasized only the role played by the quality of the metal surface and by the different elements contained in the liquid from which hydrogen had been evolved. Additions increasing the rate of penetration of hydrogen into iron were as follows: Se, Te, As, Hg, S, P.

Another method frequently used for the study of hydrogen penetration into steel, consists in the mechanical testing of specimens treated by hydrogen. Penetration of hydrogen produces compression stresses and greatly reduces the ductility of steel *).

The mechanical testing method has been used by Ludwik [5], Bardenheuer and Ploum [6], Zapffe and Haslem [7], Hobson and Sykes [8], and others. Hobson and Sykes reported that the electrolytic method of introducing hydrogen into test specimens was erratic, but failed to explain why this was so. Zapffe and Haslem used the bend test for studying the effect of

*) The harfmul effect of hydrogen on steel is therefore commonly called „hydrogen embrittlement".

adding organic inhibitors to the acid solution for pickling steel. This test revealed the fact that some inhibitors caused embrittlement of steel owing to an increased penetration of hydrogen. On the other hand, some compounds at certain concentrations decreased the rate of hydrogen diffusion during pickling.

The mechanism of hydrogen diffusion through iron and steel has not yet been elucidated. Undoubtedly, molecular hydrogen is not able to penetrate the iron lattice but there is a difference of opinion as to whether hydrogen in iron exists in atomic or in ionic form, and whether it is able to diffuse through the iron lattice or along the slip planes or only along the block boundaries or grain boundaries.

Wever and Pfarr [9] reported that the lattice parameter of an iron cathode saturated with hydrogen was 2·8614 *A* whereas the normal value for ordinary iron is 2·8610 *A*. They found that the linear expansion of the iron lattice was 0·12 %, this being due to the absorption of 1 at.% hydrogen in solid solution. Lihl [10] contested the correctness of this result. He suggested that the changes observed in the value of the lattice parameter were a secondary effect of intergranular corrosion. In turn, Lihl's view has been contested by Glikman and Sneshkova [11].

Differences of opinion exist also concerning the influence of the composition of the liquid from which hydrogen has been evolved, and concerning its rate of penetration into iron. Bodenstein [1] related this effect to the phenomenon of overvoltage, since elements or groups which raise the hydrogen overvoltage, raise the rate of diffusion of hydrogen into iron as well. Another view has been expressed, for instance, by Kuznetsof and Iofa [12]. They state that the addition of thiourea, which increases the rate of penetration of hydrogen into the iron cathode during the electrolysis of hydrochloric acid, causes the formation of hydrogen bubbles of a smaller diameter in comparison with pure acid and acid containing typical inhibitors. The values of bubble diameter were noted as follows: 0·1 mm for a pure solution of 1 N hydrochloric acid, 0·06 mm for a solution containing thiourea, and 0·66 mm for a solution containing an inhibitor.

The aim of the present work was to elaborate a method which would enable us to give a precise evaluation of the effect of adding diverse compounds to the liquid and also to determine the rate of the penetration of hydrogen into the iron cathode during electrolysis, with the purpose of elucidating the nature of this interesting phenomenon. The results of the preliminary experiments only will be presented here.

We stated that a very convenient method for the study of hydrogen penetration into iron and steel consists in measuring the linear expansion of a fine wire submitted to the action of nascent hydrogen. An arrangement suitable for this purpose is shown in Fig. 1. The given wire "*w*" with a diameter of 0·5 to 0·8 mm and 100 to 500 mm in length was kept in a suitable vessel "*v*" at a constant temperature and submitted to the action

of a load (about 2 kg per mm²). The elongation of the wire could be observed on a scale "*s*" by means of a mirror "*m*" and a lamp "*l*". The wire acted as a cathode in the acid solution, usually in 1 N H_2SO_4. The anode was made of platinum wire "Pt".

Some examples of the results obtained when using the above described method are given in Fig. 2 and 3. Curve 1 in Fig. 2 presents, as a function of time, the linear expansion of a wire of ordinary annealed mild steel (0·5 mm in diameter) treated during 310 minutes in pure 1 N H_2SO_4 at 3° C. The rate of elongation due to hydrogen diffusion was relatively small. It hardly rose after the addition of 1 g thiourea per litre solution in the 311th minute ("th.u."). The lowermost curve 2 in Fig. 2 represents the behaviour of the wire treated during 130 minutes in 1 N H_2SO_4 containing 0·16 g dibenzyl sulphoxide per litre. The wire still showed no elongation but, after the addition of the first portion of 1 g thiourea per litre solution, the rate of elongation rose a little. The second and the third addition of thiourea had no effect. The upper

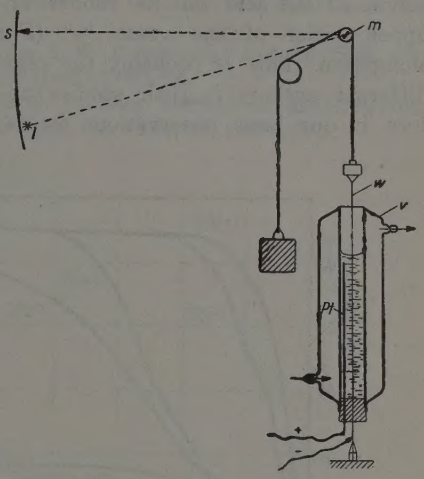

Fig. 1. Arrangement for the measurement of expansion of iron wire during electrolysis of acid solutions

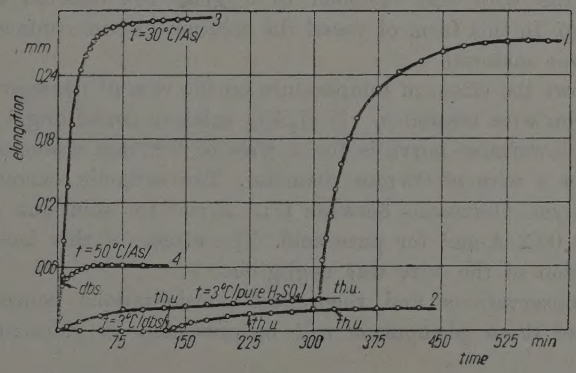

Fig. 2. Curves of expansion-time obtained in different conditions

curve 3 in Fig. 2 is for acid with the addition of 1 g As_2O_3 per litre at 30° C. Curve 4 shows, as a function of time, the elongation of the wire in the same solution containing *As* at 50° C, but 5 minutes after the

beginning of the electrolysis 0·1 g dibenzyl sulphoxide per litre solution was added. This caused an immediate decrease in the rate of expansion. We stated that very small addition of various organic compounds had the same effect as dibenzyl sulphoxide. For instance, the products of the action of the acid on the rubber or wooden cork used for stopping the upper outlet of the vessel "*v*" (Fig. 1) likewise lowered the rate of elongation. This is probably the reason for the fluctuations observed by different authors in their studies on hydrogen diffusion into iron. Therefore in our later observations we used another arrangement in which the

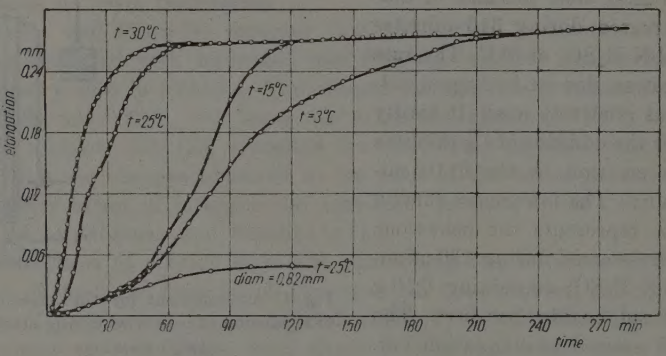

Fig. 3. Curves of expansion-time obtained at different temperatures for wire of 0·5 mm diameter (upper curves) and for wire of 0·82 mm diameter (lowermost curve)

lower end of the wire was fastened to a glass rod inserted into vessel "*v*" from the top. In this form of vessel the solution had no contact whatever with any organic material.

Fig. 2 shows the effect of temperature on the rate of penetration of hydrogen into iron wire treated in 1 N H_2SO_4 solution containing 1 g thiourea per litre. The lowermost curve is for a wire of 0·82 mm diameter, and the other curve for a wire of 0·5 mm diameter. The cathodic current density during electrolysis fluctuated between 0·15 A/cm² for solutions containing inhibitors and 0·62 A/cm² for pure acid. The effect of this factor on the rate of expansion of the wire was negligible.

Further observations and theoretical considerations concerning our investigation of these phenomena will be presented in subsequent notes.

REFERENCES

[1] Bodenstein M., Zeitschr. für Elektrochem. **28** (1922), 517.
[2] Borelius G., Metallwirtschaft **8** (1929), 105.
[3] Baukloh W., Zimmermann G., Archiv für das Eisenhüttenwes. **9** (1936), 459.

[4] Baukloh W., Retzlaff W., Archiv für das Eisenhüttenwes. **11** (1937), 97.
[5] Ludwik P., Zeitschr. des Vereins deutscher Ing. **70** (1926), 379.
[6] Bardenheuer P., Ploum H., Mit. des K. W. Eisenforsch. Inst. **16** (1934), 130.
[7] Zapffe C. A., Haslem M. E., Amer. Inst. Min. Met. Eng., Techn. Publ. No 1954, Met. Techn. **13**, (1946).
[8] Hobson J. D. and Sykes C., Journ. of the Iron and Steel Inst. **169** (1951), 209.
[9] Wever F. and Pfarr B., Mit. des K. W. Eisenforsch. Inst. **15** (1933), 137.
[10] Lihl F., Archiv für Metallkunde. **1** (1946—1947), 16.
[11] Glikmann L. A., Sneshkova T. N., Żurn. Techn. Fiziki **22** (1952), 1104.
[12] Kuznetsov V. A., Iofa Z. A., Żurn. Fiz. Chim. **21**, (1947), 201.